PTK 51163

Cultured Neuron Probe

Contract No. N01-NS-3-2393

Quarterly Report Nos. 5 and 6

May 1, 1994 - October 31, 1994

California Institute of Technology

Hannah Dvorak

Michael Maher

Jerome Pine

Steven Potter

Yu-Chong Tai

John Wright

Rutgers University

Anatol Bragin

Gyorgi Buzsaki

This QPR is being sent to you before it has been reviewed by the staff of the Neural Prosthesis Program

General Introduction

Our aim is to develop a cultured neuron probe. This consists of a silicon structure into which individual dissociated neurons can be placed, and which can be inserted into an intact nervous system. Furthermore, within the structure each neuron is in close proximity to an electrode, by means of which it can be stimulated, or its activity can be recorded, through electrical leads which connect to external electronics. It is hoped that neurons in the probe will synaptically integrate with the host nervous system, to provide a highly specific, relatively non-invasive, two-way communication channel. If this occurs, the methodology has important possibilities for neural prostheses. The goal of this project is to perform initial experiments to establish the feasibility of communication by means of a neuron probe. The tissue we have chosen in which to initially implant the probe is the rat hippocampus. If initial studies are successful, probes will be designed and implanted for communication with sensorimotor cortex.

The neuron probe we plan to fabricate will be made of micromachined silicon and will have sixteen electrodes: one conventional electrode to detect activity during placement of the probe, and fifteen within wells into which neurons will be placed. Its configuration will be similar to that of passive multielectrode probes which have been developed. It will be implanted when the cultured neurons are very young, and after a time of weeks it is hoped that they will have survived and made two-way synaptic connections. By stimulation and recording in the host and probe, we will test for the existence of such connections. An essential feature of the experiments is that the viability of the implanted neurons will be independently determined over time by stimulating them and recording their resulting action potentials.

Summary

Neurochips

A major effort has been made to understand and improve on the low yield of growing neurons from wells. Culture conditions have been refined so that "control neurons" not in wells grow well and exhibit good survival for several weeks in culture. Studies of different grillwork materials and configurations during this period have finally led to what we believe will be a design in which well neurons grow out in large numbers, comparable to outgrowth of controls.

Work with SCG neurons confirmed that those that did grow out of wells had long term survival comparable with control neurons. During tests of different transparent grillwork materials, for better visibility of cells in wells and also for using voltage sensitive dyes for recording activity, good outgrowth was seen for a batch of test chips with silicon dioxide grillwork. It was also observed that outgrowth was poor from chips with silicon nitride grillwork. Because the grillwork was transparent it could be seen that there was an overhang of about one micron around the edges of silicon nitride wells, far more than had been expected from the EDP etch. However, the silicon dioxide grillwork had regions of no overhang, an artifact resulting from a wet etching process. This led to studies of possible overhang in the old silicon grillwork chips, which revealed serious overhang problems. A new nitride grillwork design was then developed, with zero possible overhang, and very good outgrowth was then observed in test chips with the new grillwork.

Further work with SCG neurons has resulted in improved DiI staining, and also the use of calcein AM stains for easily assessing the viability of cells in wells. In addition, a system for making timelapse movies of early outgrowth was developed, which verified directly the escape of neurons out of the corners of wells. The new no-overhang grillwork design also embodies a reduction in the size of the corner openings, and a corresponding increase in the central opening, which was marginally small for SCG's.

Work with embronic hippocampal neurons confirmed, with new test wells, that the no-overhang design led to approximately 70% outgrowth, comparable to that for "control" cultures. In order to make timelapse movies of hippocampal neurons possible a system of medium control and a new precision temperature controller were developed.

Dummy neuroprobes

The existing stock of dummy neuroprobes for *in vivo* tests all have silicon grillwork, with overhang that makes outgrowth problematic. In order to make it possible to use these, methods were devised for reprocessing them so as to eliminate the overhang. This is a very labor-intensive task, but some probes have been modified so that ongoing *in vivo* studies can proceed while new no-overhang probes are fabricated.

Hippocampal slice cultures

The major effort has been to proceed to the stage where loaded dummy probes, with DiI stained neurons, can be placed in contact with slices, and outgrowth into the slice can be monitored with fluorescent microscopy. This has entailed the development of DiI staining methods which are not only effective for staining neurons but which produce minimal background staining of the dummy probes and eventually of the slice. The results are encouraging, and probe-slice experiments will soon begin. In addition to staining studies, ancillary work has involved development of an improved procedure for loading stained neurons into probes and also the development of a high speed video system intended ultimately for recording probe-slice physiological integration with voltage-sensitive dyes.

Fabrication

Early in the period covered by the report, fabrication methods were refined so that improved photolithography in the recess where wells are

patterned has been achieved. Following the discovery that grillwork overhang might be the problem leading to poor outgrowth, studies were made of the silicon grillwork of the existing dummy probes and nurochips, and the cause of the overhang was understood. A new design with silicon nitride grillwork was created, which has no possibility of overhang. New masks were made, and test chips fabricated. The encouraging results, noted above, have resulted in the decision to adopt this design and to fabricate as quickly as possible a new batch of dummy probes for *in vivo* and slice experiments.

In Vivo Studies

Fixed brains from rats which had been impanted with dummy probes loaded with septal neurons were analyzed by sectioning, cholinestesterase staining, and looking for stained axons emerging from the probe region. In two of five rats sacrificed 4-6 months after the probes were implanted stained axons were observed. The outgrowth was good, and the very low yield is thought to be the result of the overhang problem discussed above.

In addition, studies of the observability of DiI stained neurons were conducted. Small low-density grafts of stained neurons were made, and it was found that stained cells were visible one month after transplantation. However, background staining was a problem. It is hoped that the methods developed for slice experiments will lead to transplants with much less background staining in future.

Neurochips

Significant progress has been made in tackling the issue of poor process outgrowth from neurochips and neuroprobes. Most importantly, we discovered that our entire inventory of neurochips, neuroprobes, and dummy chips have a significant overhang of the grillwork over the sides of the wells. The figure below illustrates a neuron in a well with overhang on the right edge and no overhang at the left. The neuron is in intimate contact with the sides of the well, and the growth cone is typically very flat - - approximately 2-3 μm in diameter but only 0.1-0.2 μm thick. Thus, when the growth cone encounters the overhang, no part of it will extend over the barrier and the cone will not be able to establish a foothold beyond the well.

In the following sections, work with both SCG neurons and hippocampal neurons will be described which provides evidence for this supposition. Furthermore, initial experiments with a new no-overhang grillwork design indicate that good outgrowth will be obtained.

Previously, the extent of overhang was unclear, but it was assumed to be much less than 1 μm wide, and to have little effect on the cells. Close inspection revealed instead that the EDP etch regularly generated 1 μm overhang. Furthermore, growth cones on SCG's and hippocampal pyramidal cells are so thin that it is entirely possible that the growth cones, upon encountering the overhang, essentially see an insurmountable wall. In order to bypass the overhang, growth cones would have to bend through an angle of approximately 135°. While we have not investigated this phenomenon in detail, our failure to obtain regular, robust growth of processes out of overhung wells suggests that the overhang blocks growth cones.

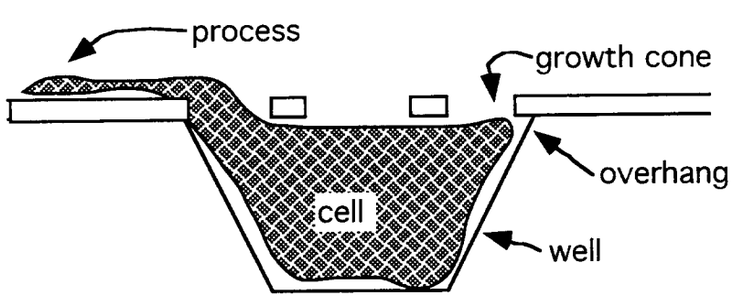

Work with SCG neurons

Outgrowth and long-term survival on different chip designs

In the past months, we have continued the practice of leaving neurochips undisturbed on the microscope stage for about two hours following the loading of cells into wells, in order to allow the cells to attach to the substrate sufficiently that they are not dislodged when the chip is then moved to the incubator. SCG neurons are loaded into the wells in an air medium, which must be replaced with CO_2 medium for long-term incubation. SCG neurons also require several hours to attach strongly to the substrate. To prevent washing cells out of the wells, the medium is not changed for 12 hours after loading cells.

Using the coating protocol of an overnight soak in 1 mg/mL poly-L-lysine, followed by UV sterilization and a 2.5 hour application of laminin, we had consistent outgrowth from our old batch of neurochips, but with a fairly low number of cells growing. In nine preparations that were otherwise successful (i.e. cells on the chips outside of the well area were growing normally), two to eight neurons eventually sent processes out of the wells, with an average of 4.2 wells showing processes after a day of growth. The top figure on the following page shows SCG neurons, stained with DiI, on an old neurochip after two days in culture. There are many stained cells in wells, but only clear outgrowth from a corner of one well, in row 2, column 4. Assessment of outgrowth after more than a day in culture is problematic, because processes that originate outside the well area, as well as from wells, often grow into other wells (as seen in the video we made of SCG outgrowth on a dummy chip). To tackle this problem, we are attempting to improve process and cell body visibility by fluorescent staining.

Some encouraging results in long-term survival were seen on the old neurochips. In one case, thick dendritic processes, characteristic of mature SCG neurons, could be seen coming out of five wells after 12 days in culture, as shown in the second figure below. The "plaid" background pattern is an artifact of etching the boron-doped silicon etch stop layer (now eliminated with boron-germanium doping). The dense process growth is characteristic of old

SCG cultures, and comes from cells outside the wells. Three wells on this chip still had thick processes after 16 days in culture.

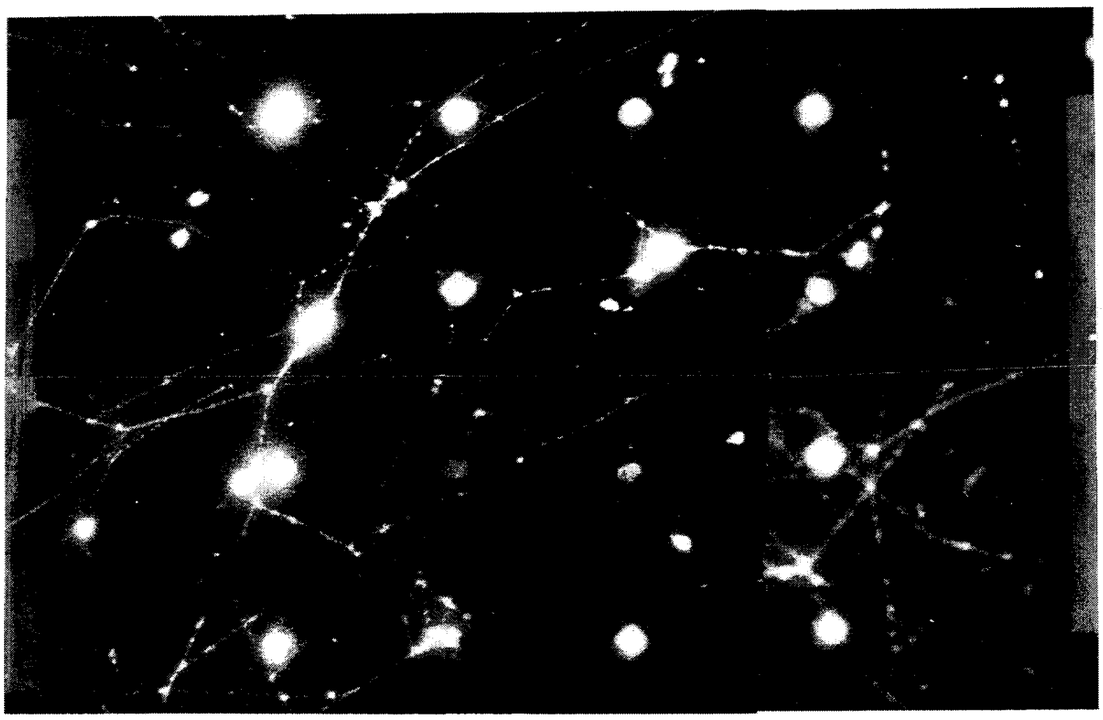

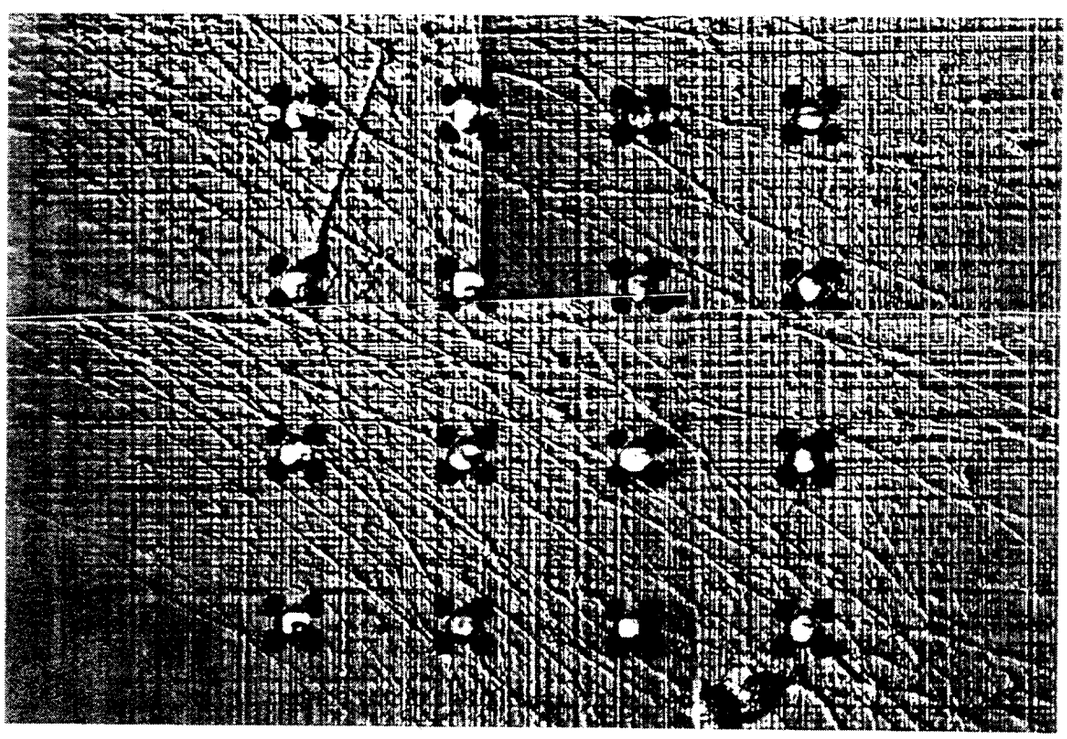

The chips with silicon dioxide grillwork had a much smaller and more variable overhang, including areas with no overhang whatsoever. Outgrowth on these chips was better, though still variable. In four experiments, we saw as few as two or as many as 15 neurons out of 16 wells sending out processes after a day in culture. The figure below shows excellent outgrowth in such a culture after two days. Long-term survival was also seen on these chips. In one case, after 37 days in culture, three wells of an oxide-grillwork chip had thick (>5 μm) dendrites growing out of them.

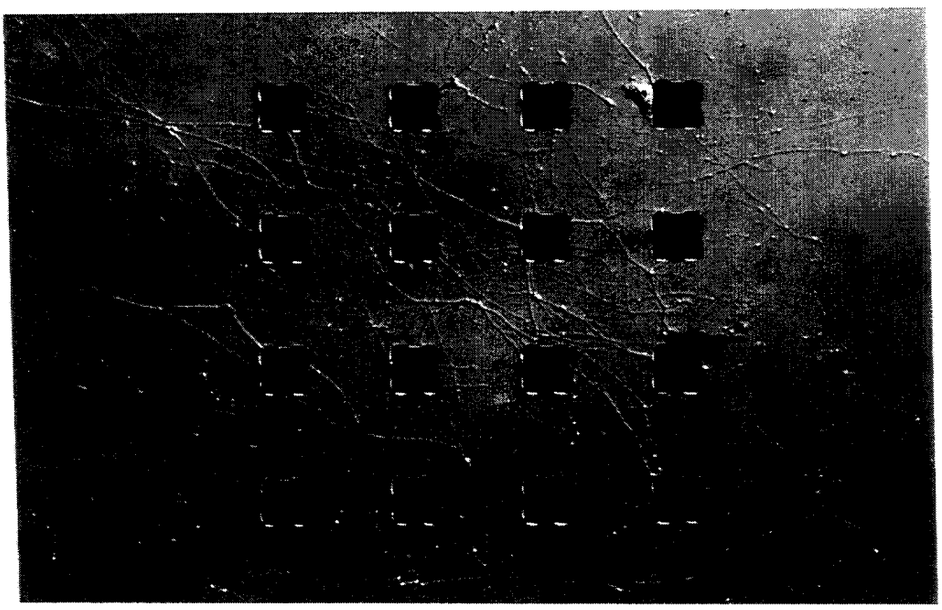

Finally, a new grillwork design was devised, described in detail in the fabrication section, in which an overhang could not possibly form. Preliminary results with dummy chips of this type are extremely encouraging. The first such chip that was loaded with SCG neurons had outgrowth out of 10 wells, shown in the figures on the following page. The upper photo has etching artifacts on the silicon; and the sketch below shows a more clear tracing of process outgrowth. The other six wells were empty after a day (suggesting that neurons never attached in these wells). A second chip, of which a video of neuron outgrowth was made, had nine neurons grow. The most recent attempt resulted in three cells growing from the only occupied wells, with six empty wells and three cells visibly escaping from wells. The current grillwork design results in unusually large corner holes, through which immature SCG neurons can easily move. This grillwork design has been modified for the next production run.

A maximum of 50% outgrowth, while encouraging, is still not as much as we'd like. On chips in which we could see into the wells (the flat-bottomed design), we could track the fate of the neurons loaded into the wells by direct observation. While some neurons did still escape from wells (as determined by the presence of the empty well and a growing cell nearby on the top surface of the neurochip), many cells could be seen to stay intact in wells and not to grow, followed by disintegration of the same cells into debris after a few days. The table following shows the distribution of cell fates after a day or two in culture in several chip experiments.

Survey of observations of neurochip wells one day after loading with SCG neurons.

Chip, date	Empty	Escaping	Growing	Intact, not growing	Full of debris
MF5, 6/28	4		3	5	1
MF11, 7/6	2	1	8	5	
MF5, 8/17	2	1	4	1	8
MF5, 8/24	3		2	5	6
MF11, 8/25	5		2	12	1

Thus, it would seem that many apparently healthy cells failed to send processes out of wells. Generally, the wells that contained intact, non-growing cells were subsequently observed to be full of debris or empty; this suggests that the cells die if they fail to grow. Some neurons that do send out processes die as well, as do neurons that aren't in wells.

As discussed above, SEM observations of the neurochips revealed an overhang of as much as several microns over the edges of the wells on the old batch of chips; it seems that this overhang was sufficient to hinder neuronal process outgrowth. Subsequently, three new chip designs were implemented. The first batch, with silicon nitride grillwork, still had substantial overhang. In two experiments, seven and two SCG neurons respectively grew out of wells after a day in culture.

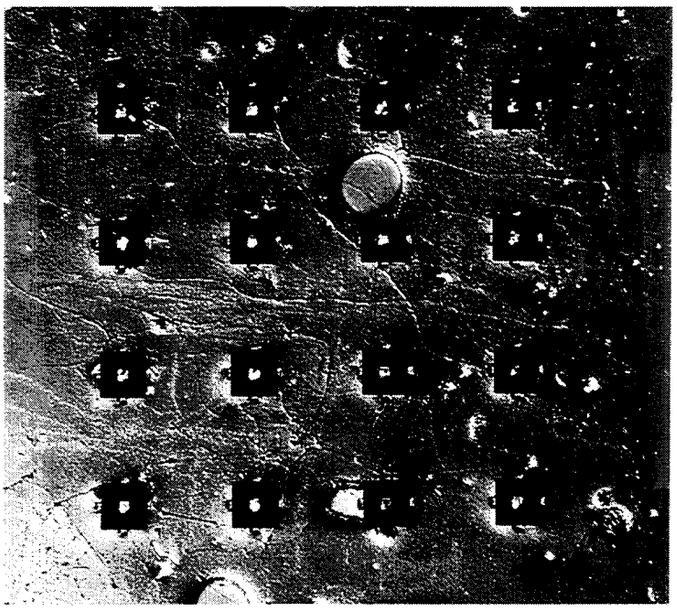

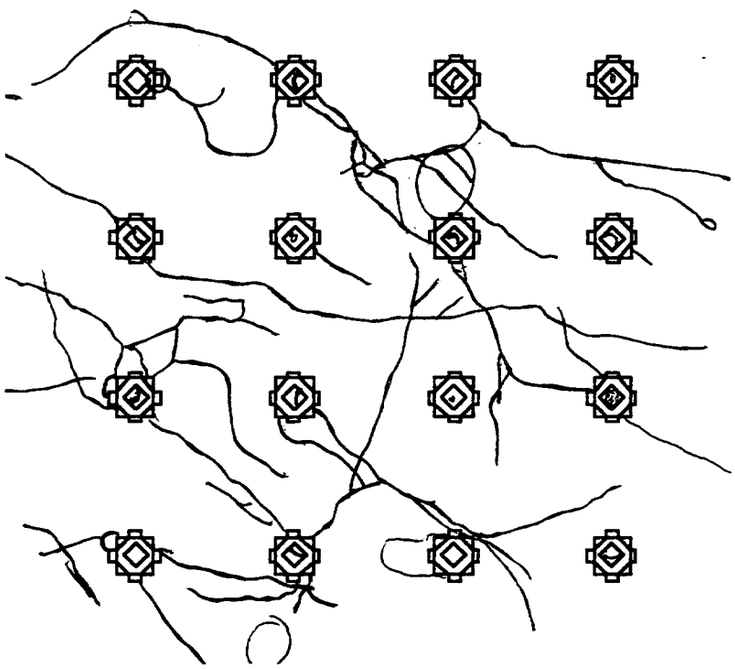

Neurons growing out of two chips, one with oxide grillwork and the other with the new grillwork, have been fixed and mounted for an SEM study that will show just how the growing processes do navigate their way out of the wells and possibly around the overhang.

Staining of SCG neurons for better visibility

As mentioned above, one problem in assessing the extent of successful outgrowth of neurons from wells is the rapid proliferation of processes from cells outside the well area. It would be valuable to at least limit the problem by being able to distinguish processes arising from cells in wells from those that come from cells outside. Several different staining protocols have been tried or considered:

1. Evaporating DiI into the wells so that growing cells incorporate the dye into their membranes and label their processes. Unfortunately, tests of neuron growth on evaporated DiI showed very poor survival and no staining.

2. Staining cells with DiI after they have been put into the wells and started growing. We have not yet come up with a successful protocol for injecting a sufficiently small volume of DiI solution into the well area without either staining all other cells as well, or killing the cells of interest.

3. Staining cells with DiI in suspension before loading them into wells. This has been done successfully with hippocampal neurons (described below); however, SCGs seem to be very sensitive to DiI toxicity. We are currently working on a modified, gentler protocol for SCG staining.

Another problem addressed by staining is long-term survival in wells, particularly those in which the cells are not visible (i.e. dummy chips without a flat bottom, such as the oxide-grillwork chips). A lipophilic dye such as DiI is not very useful for this purpose, because in addition to staining cell membranes, it is also picked up by cellular debris such as that left behind in a well by a dying cell. An alternative is to use a vital stain such as calcein AM (Molecular Probes), which is taken up and hydrolyzed to the fluorescent calcein by cytosolic esterases; therefore, only viable neurons are stained. When used at sufficiently high concentrations (5-10 μM), this dye will stain thin processes as well as cell bodies; however, to enhance cell survival, concentrations low enough (1-2 μM) to stain only cell bodies and thick processes (dendrites) are used.

Using the calcein AM stain, we found that in mature cultures, the presence of thick dendritic processes is reliable evidence for the presence of a healthy

neuron in a well. By about two weeks in culture, the vast majority of SCG neurons have several thick dendrites. The oxide-grillwork chip described above was stained with calcein AM after 37 days in culture; only the three wells that had thick processes growing out of them lit up, even though a lot of thin processes were coursing throughout the well region and coming in and out of wells. Dendrites from wells in this culture are shown in the figures following, one by Nomarski illumination and the other with fluorescent calcein.

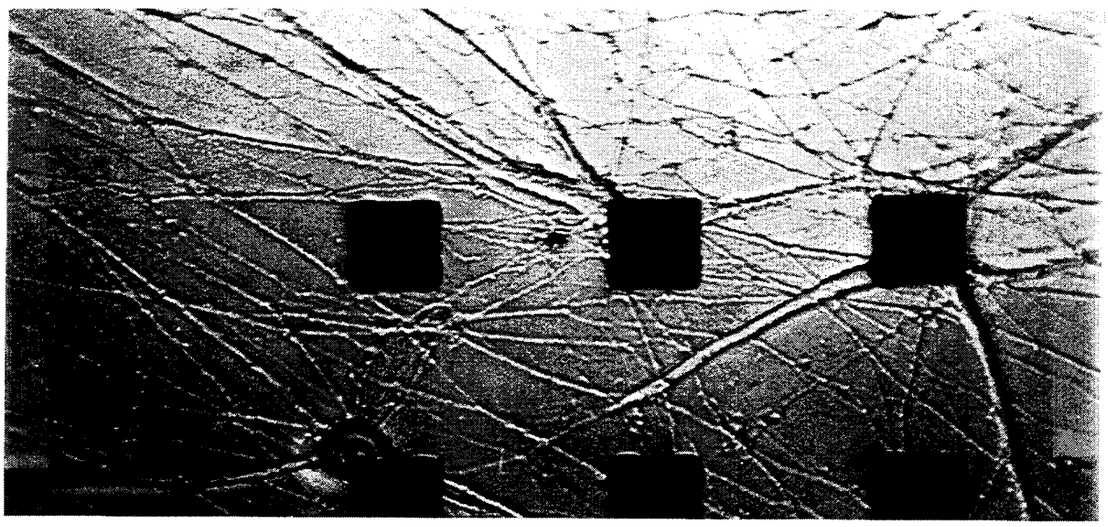

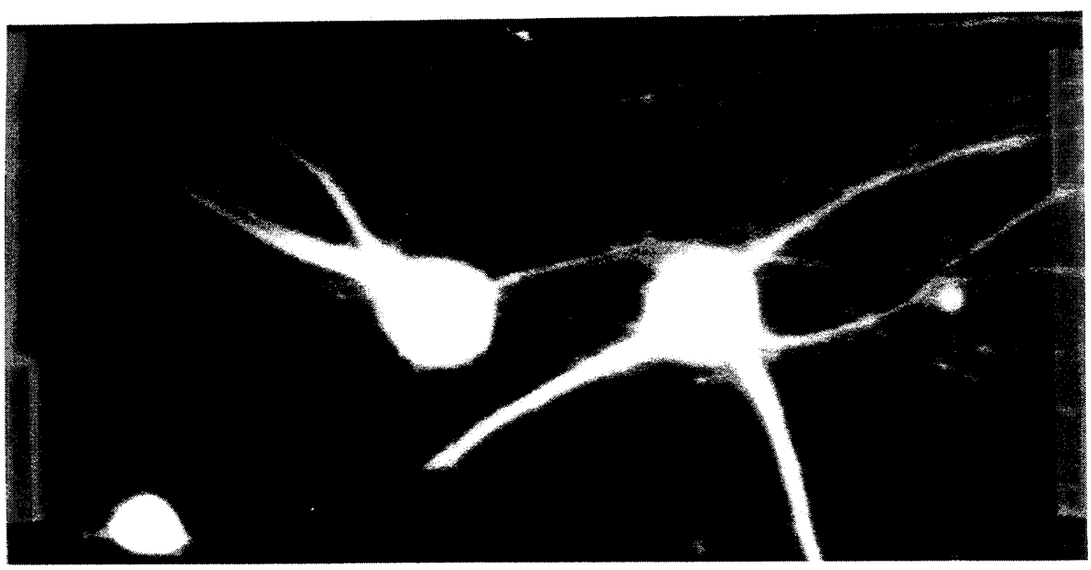

Time-lapse videos of SCG processes emerging from wells

Using a Sony CCD camera attached to the camera port of the upright microscope, a standard VHS VCR with a custom-built time-lapse timer, and a frame grabber on a Macintosh computer, we were able to generate time-lapse videos of cell growth. We can obtain movies directly on video tape, with any desired length and scaling factor, as well as movies limited to fifty frames on computer. The video tape system has the advantage of indefinite length, indefinite speed-up, and high time-resolution to observe changes on the order of seconds. It has the disadvantage that the contrast of growth cones and processes is low and they are difficult to see without video enhancement . The computer system has the advantage of high-grade post-processing software to enhance contrast, but the disadvantage of a limited number of frames with which to make a movie. Thus, long-term computer-enhanced videos can only be made at the expense of limited time-resolution.

Videos were made of the processes of an SCG neuron emerging from a new-style, no-overhang well. The chip was prepared in the standard method, with poly-L-lysine and laminin coatings on the oxidized silicon surface. The wells were loaded at room temperature with the dish lid off. After loading, a large glass cover slip was sealed to the dish using silicone vacuum grease, so that evaporation of the medium would not affect the microscope focus or alter the medium concentrations. The dish was then heated to 37 °C and maintained at that temperature using a heater block and the temperature controller described in the Appendix to this report. Frame-grabbed and VCR videos were taken of the growth of cells on this chip for 12 hours. Six frames of the frame-grabbed video, spaced approximately 30 minutes apart, are shown in the figure on the following page. (When action on the video is enabled, the motion of the processes makes them much easier to see.) Growth and motion of the processes is continuous and fairly rapid, with obvious micron-sized motions detectable on the several-second time scale.

In Figure a], taken soon after the well was loaded with an SCG neuron, a process emerging from the right side of the well is faintly discernible. Over the next few hours, this process extends and branches several times. By the last frame, the growth cones have extended beyond the field of view. A second

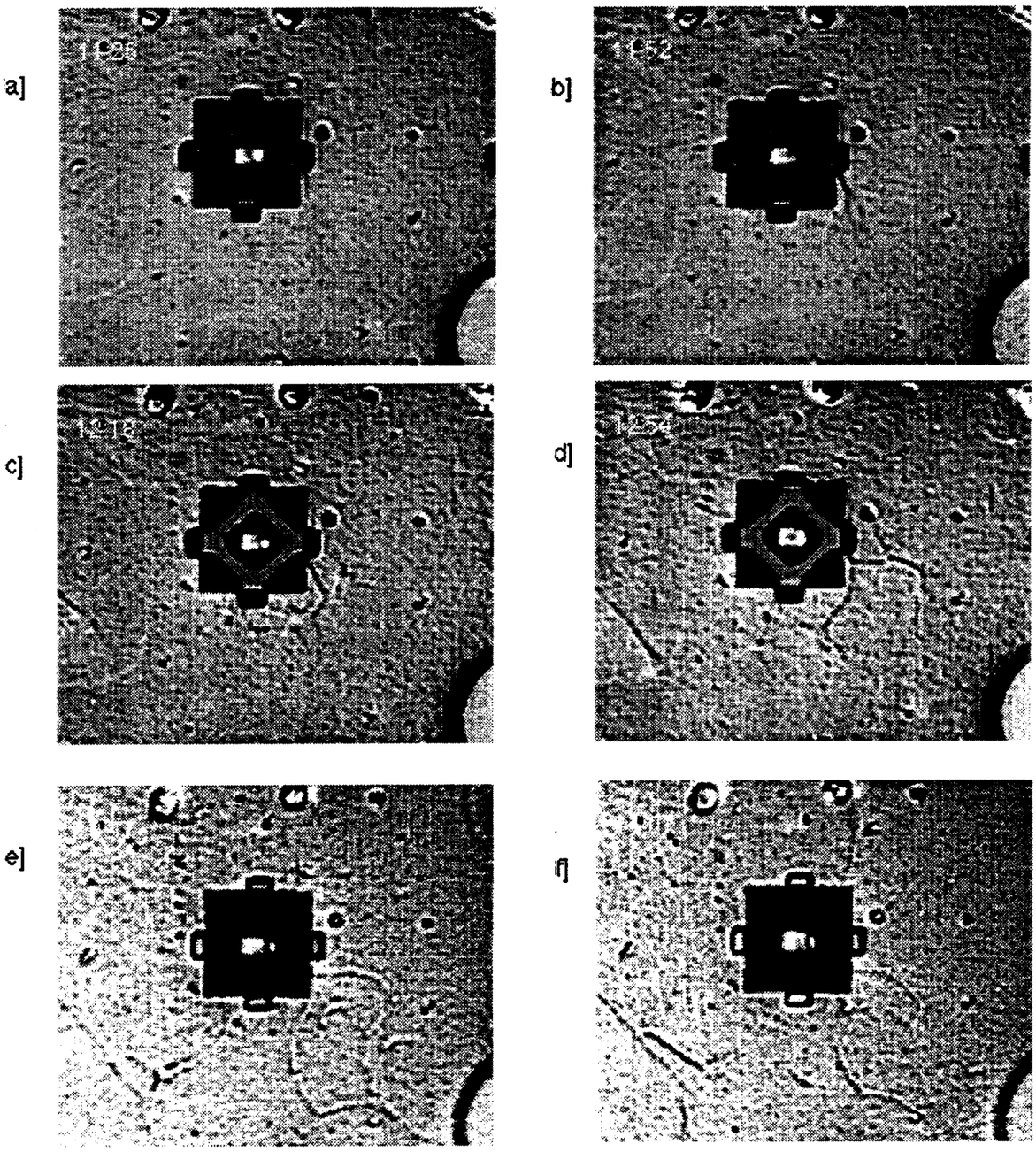

growth cone emerges from the lower edge of the well between frames c] and d], and a third process can be seen emerging from the upper right corner in frame e].

Work with hippocampal neurons

Growth from wells with no overhang

Two new-style dummy chips with no overhang , designated ND1 and ND4, were loaded with E17 embryonic rat hippocampal pyramidal neurons. The following protocol was used to mount and prepare the chips.

(1) Glued chip to bottom of 35 mm tissue culture dish with minimal Sylgard or silicone rubber. Baked at 65°C for 2 hours to cure.

(2) Removed sacrificial oxide mask with a 5 minute soak in buffered HF, followed by 10 rinses in tissue culture water.

(3) Rounded off the near-atomically sharp silicon corners with a 15 second etch in 49:1 HNO_3:HF solution, removing approximately 0.5 μm of silicon from all exposed surfaces. This was again followed by 10 rinses in tissue culture water.

(4) Oxidized silicon surfaces with a 2-hour soak in 30% H_2O_2 at 65°C. Rinsed 10 times in tissue culture water.

(5) Let soak overnight in tissue culture water.

(6) Rinse 10 times in tissue culture water. Dry in 65°C oven for one hour.

(7) Sterilize in UV box for 30 minutes.

The following protocol was used to prepare the chips for cell attachment.

(1) Soak in 95% ethanol for 5 minutes to hydrate the wells.

(2) Rinse 5 times with sterile water.

(3) Add 1 mg/ml poly-L-lysine or poly-DL-lysine in PBS at pH 7.2. Let soak at room temperature for 2 hours.

(4) Rinse 5 time with PBS.

(5) Add 13 μg/ml laminin in PBS at pH 7.2. Let soak at room temperature for 4-12 hours.

(6) Rinse twice with PBS, then twice with tissue culture medium. Allow chip to soak in medium for at least one hour before plating cells.

The new transparent silicon nitride grillwork allows for quick determination of the hydration state of the wells. Generally, the grillwork of a well full of air under water is much more reflective than a hydrated well. In addition, the corners of a well full of air have bright streaks, presumably where

the curvature of the bubble allows reflection. These streaks are absent when a well is full of water. Generally, we now check whether or not all wells are actually hydrated before introducing poly-L-lysine, to ensure that all wells will be usable later when cells are being loaded. If a well has an air bubble, a cell cannot be loaded into it, and we have not yet discovered a means of removing air bubbles other than hydration with ethanol at the beginning of the wet chemistry.

In order to completely minimize the possibility of damaging the cells when loading them into the wells, a method was developed by which hippocampal cells can be parachuted into a well without touching it at all. A feeder layer of cells is first plated onto the chip, at a density of about 500 mm^{-2}. After settling for 45 minutes, all cells are sucked up from the well region to a distance of 2 mm. Excess medium is placed into the tissue culture dish, and a second plating of 10,000 cells is performed. The dish is immediately placed under the microscope, before the cells have a chance to settle. Under normal conditions, 30-40 minutes of falling cells can be expected. As the cells fall, individuals are selected and moved into position above a well by moving a pulled pipette in the medium near the cells. Viscous drag causes the cells to follow the pipette, and micron precision in placement is possible. When the cell is directly above the well hole, it is allowed to fall on its own. Unfortunately, the current design of the central well hole has about the same diameter as a pyramidal cell, and pyramidal cells are extremely sticky. As soon as they touch anything, they stick to it. Often a cell will stick to the grillwork as it falls through, and in these cases, the it will invariably pull itself onto the top of the grillwork as it begins to grow, escaping the well. The size of the central hole has been increased for the next generation of chips to alleviate this problem.

Using this method of parachuting cells, the 16 wells of chips ND1 and ND4 were loaded with single cells. The figures on the following page show the culture ND1 after three days. Ilt can be seen that processes emerge from eight wells, and that 3 cells had escaped. Escaping cells are an issue which we have addressed in the new well design. The cell in row 2, column 3 of sits right in the upper right corner of the well, apparently having escaped there. If we assume that the 3 escaped cells would have lived had they remained in the wells, this chip had a survival rate of 11/16 = 69%, comparable to the nominal 70-80%

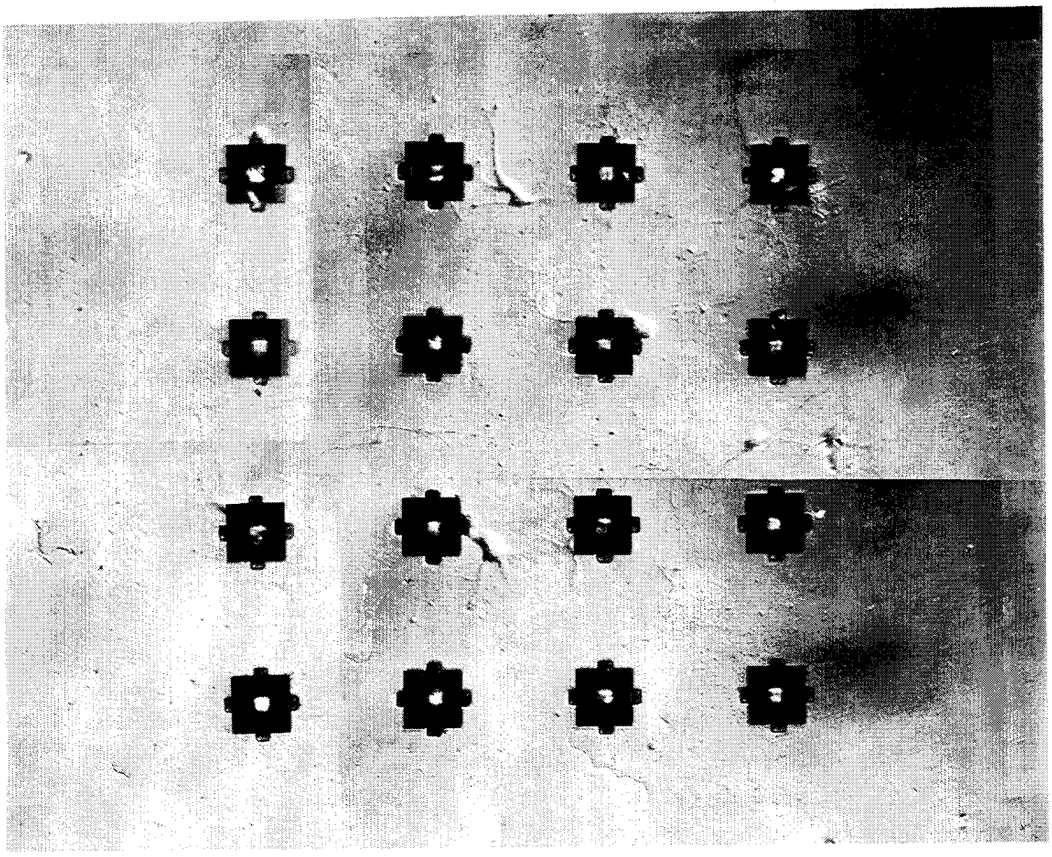

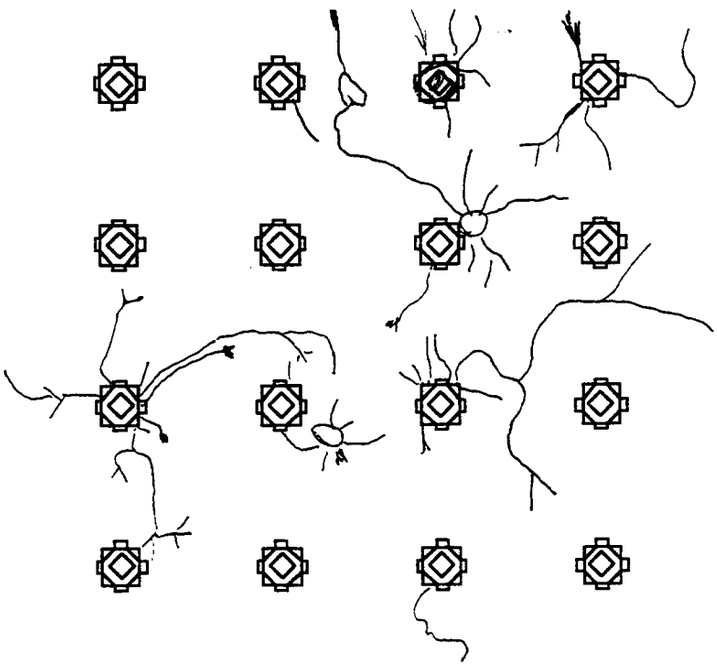

typical of flat-dish hippocampal cultures. The pair of figures below shows the same culture one day later, with copious new outgrowth.

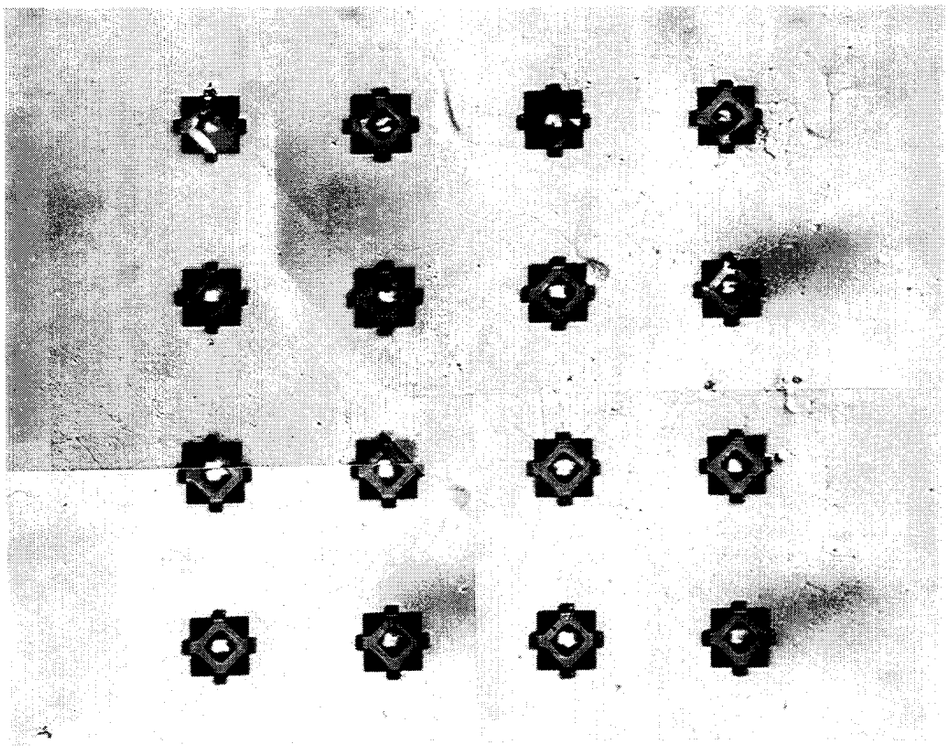

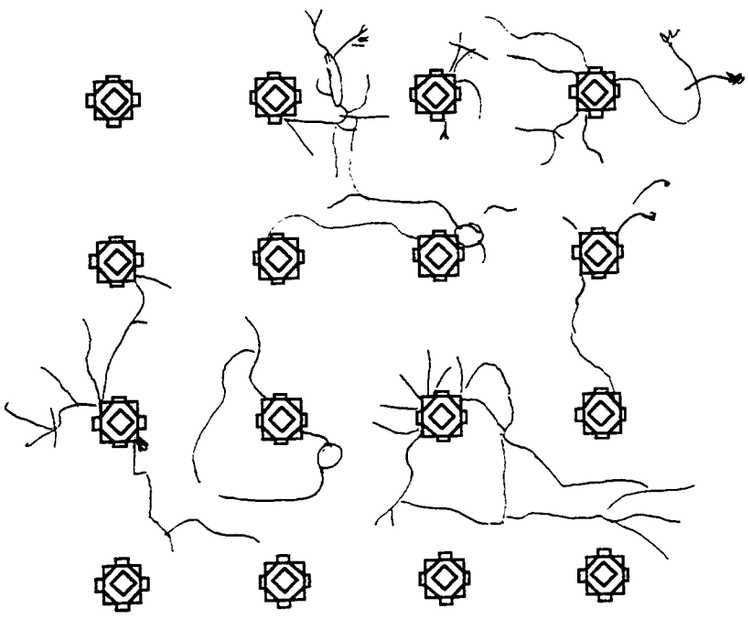

The figures below demonstrate the growth on chip ND4 at 3 days. At this point, processes emerge from 10 of the 16 wells. The overall appearance of the dendritic trees emerging from wells is similar to that of control cells on the flat part of the chip.

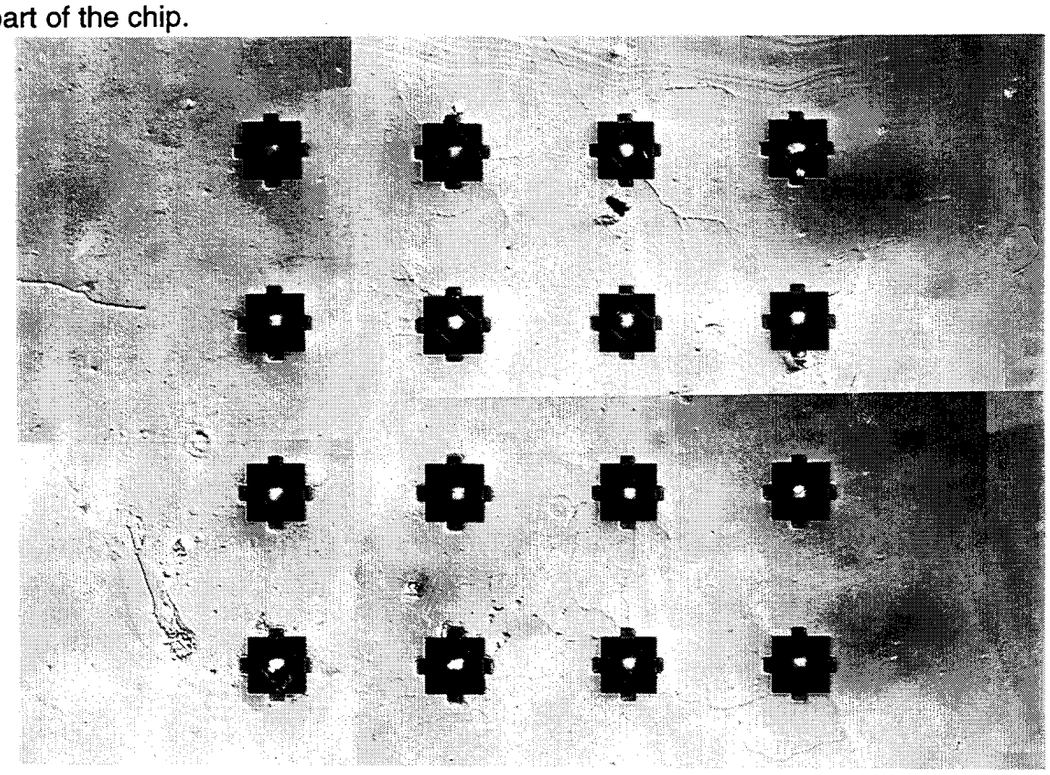

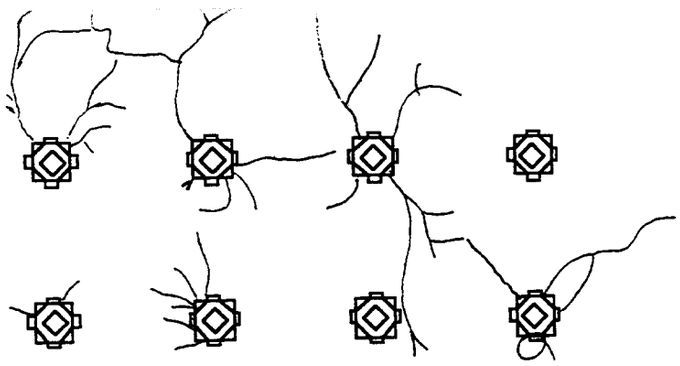

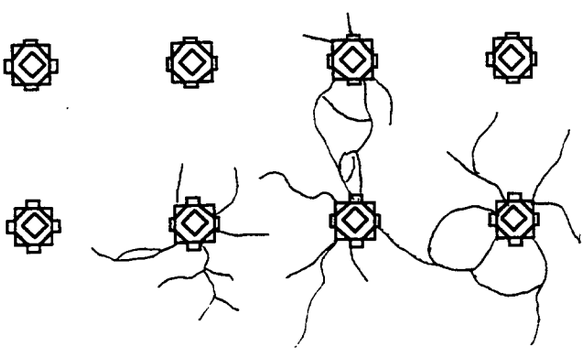

Time-lapse video

As mentioned in the previous report, we are interested in being able to recognize, immediately after dissociation, cells that will become healthy neurons, so that they may be chosen to be placed into the wells of the neuroprobe or neurochip. To this end, we have followed their growth after plating onto glass coverslips using time-lapse video microscopy. We have also used time-lapse to observe processes emerging from wells containing healthy neurons, and cells escaping.

We have made several improvements in our technology for making time-lapse videos. We have designed and built a temperature controller (see Appendix) that maintains the temperature of the culture dish on the microscope stage to within 0.1°C, preventing problems with focus drift due to thermal expansion and contraction.

We have been unsuccessful in finding an adequate air-buffered medium in which to grow the neurons during time-lapse. Drift in pH due to evaporation precludes the use of our normal Neurobasal/B27 medium, which is buffered for a 5% CO_2 environment. Thus, we have taken the approach of sealing the dishes to prevent evaporation. The pH remains constant for over 24 h, however, the dissolved oxygen is consumed within 12 h. Through the use of a dish coating (poly-L-lysine/laminin) that encourages rapid growth of hippocampal neurons, we now have ample time to observe neuronal outgrowth, as illustrated in the figures on the following page. They show two successive views taken 15 minutes and 5.5 hours after plating.

From these time-lapse studies, the great majority of cells from a dissociated E17 rat hippocampus appear to be healthy neurons. For example, of the 33 cells visible in the figure, 22 had clear processes and well-defined cell bodies. Another 6 had flat lamellipodia or wide processes, and may have been immature neurons or glial cells. Five were dead upon plating or died soon after.

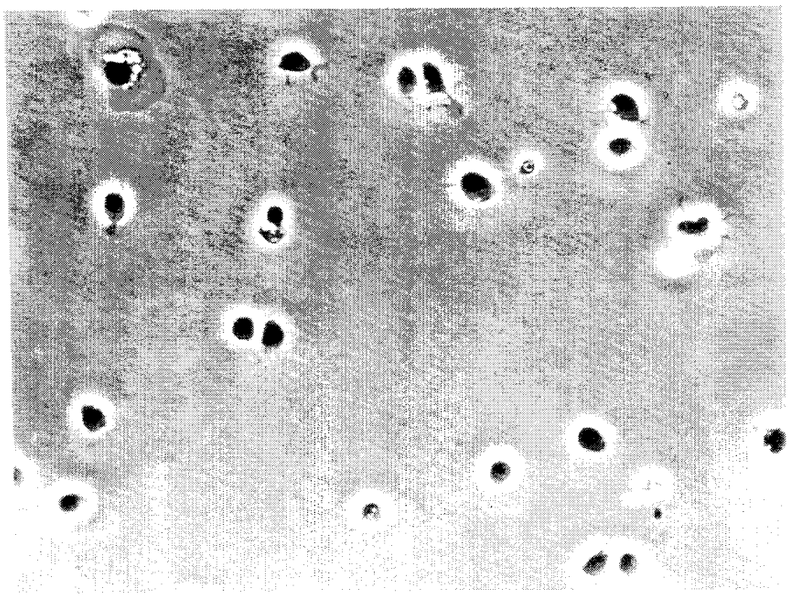

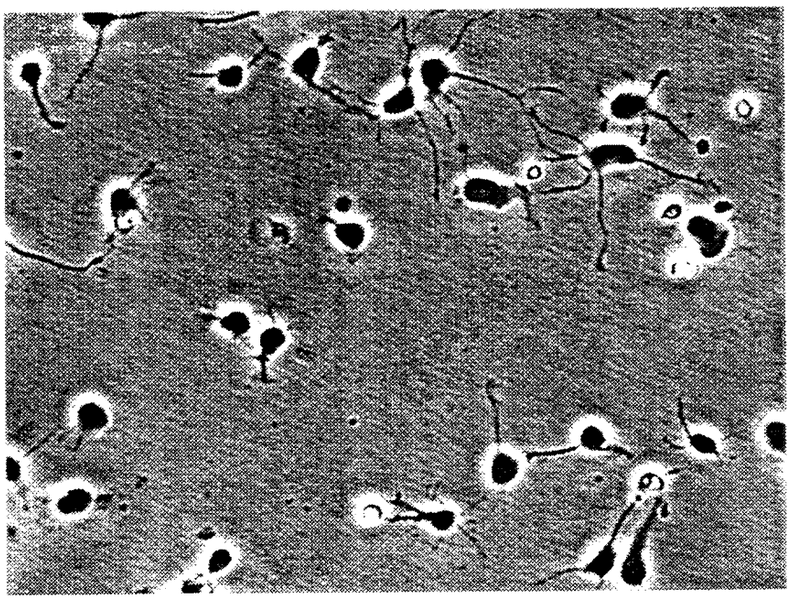

Dummy Neuroprobes with no overhang

Given that our entire current supply of neuroprobes is hampered by overhang, and that we need to proceed as soon as possible with further *in vivo* studies, we have begun investigating the possibility of remanufacturing some of the probes to eliminate the overhang until new probes become available. We have invented a method whereby the corners of individual probes are masked off by hand, and the nitride at the corners is removed by RIE. Four probes have successfully been treated in this manner, and outgrowth of processes from treated corners has been observed.

The procedure for modifying probes is as follows. First, the shaft of the probe is supported by a blank chip of silicon glued to a glass slide with silicone rubber. A minimal dab of silicone is placed on the slide next to the blank chip, and the probe is pressed into the silicone. By gently pressing the probe flat against the blank chip, the shaft is well enough supported for the remainder of the processing. After curing the silicone for 2 hours at 65°C, a drop of thin photoresist is applied to the handle of the probe and allowed to run over the shaft and the blank chip. Occasionally, we have had difficulty in getting the resist to stick to the probe. This can be resolved by cleaning and oxidizing the probe in 30% H_2O_2 at 65°C for 2 hours, then rinsing and drying.

The photoresist is allowed to dry for 20 minutes at a steep angle, allowing the resist to form a thin coat over the needle. The consistency of the resist is crucial when scraping. Before 20 minutes, the resist is runny and gummy, and will not peel cleanly from the surface. After several hours, the resist becomes too tough to scrape, and tends to come off uncontrollably in large chunks. In between, the consistency constantly changes from gummy to lumpy, and continual readjustment must be made to scrape accurately.

The probes are then placed under the microscope, with a 45° angle between the shaft axis and the micromanipulator axes. A flame-sharpened tungsten wire is used to scrape the resist away from the corners of the wells. Great care must be taken in exposing the nitride only at the corners. With practice, it is possible to scrape away the resist at the corners without touching

the rest of the grillwork. It is also important to scrape away resist up to several microns away from the well, so that any residue left behind does not block the RIE. The point at which the resist is completely removed from the nitride is easily determined, since the nitride surface is mirrorlike while the resist-coated nitride appears dull and diffuse. About 1-2 hours are required to remove the resist at all corners of 16 wells, making this method unsuitable for mass-production.

The probes are then etched for 8 minutes in a plasma consisting of SF_6 and O_2, etching approximately 3000 Å of Si_3N_4. After etching, ghosts of the overhang remain in resist. Determination of etch completion should be made by the grey appearance of exposed silicon, not by the presence of overhang-like structures. The resist is then removed by soaking for 30 minutes in acetone, then 5 minutes in piranha etch (6 parts H_2SO_4 and 1 part H_2O_2), followed by 10 rinses in distilled water. The figure below shows one well of a nitride dummy chip which has had two corners freed of overhang using this procedure. The two etched corners clearly have no overhang, with bare silicon at the corners. The other two corners remain as they were initially, with approximately 1 μm of overhang surrounding the entire well edge.

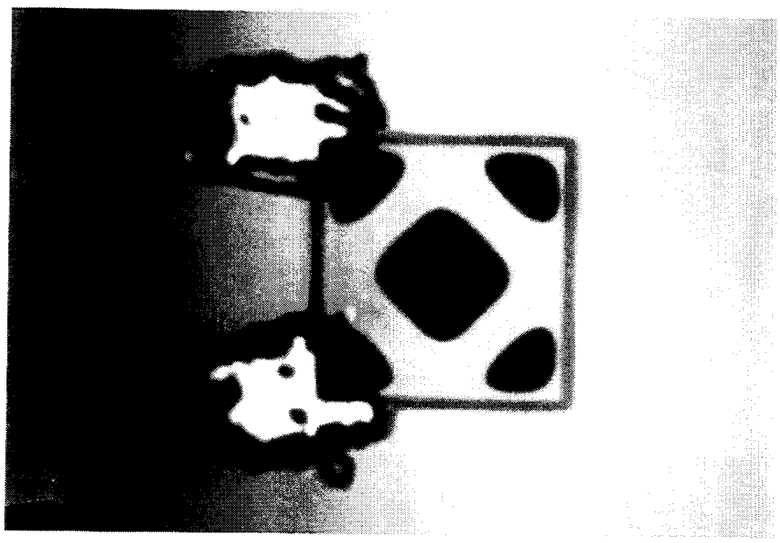

One such probe, DP3, was loaded with hippocampal pyramidal cells. Only 7 of 15 wells were loaded; the remainder were filled with air. Of these seven, two grew from the wells and 4 escaped through the center holes, due to sticking as they parachuted through. The figure below is a photomicrograph of this probe at 2 days after loading the wells. Unfortunately, the masking method makes the edges of the nitride quite unsightly, and complicates the image. Processes can be seen to emerge from the areas near the etched corners of two of the wells. It appears that our historic problems in getting sufficient growth from neurochip and neuroprobe wells arise almost entirely from the overhanging grillwork. All current studies on chips and probes with no overhang, whether by design or by remanufacture, suggest that neuronal outgrowth is no longer significantly affected by containment in a well.

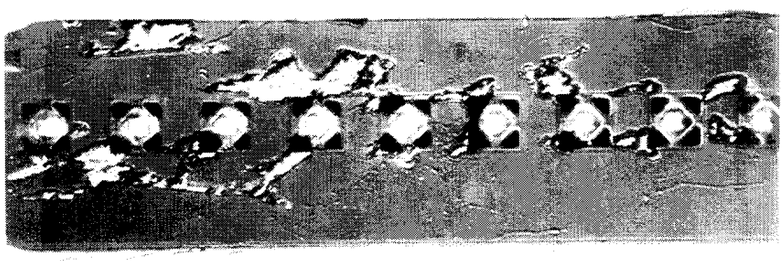

Hippocampal Slice Cultures

Staining

Our goal of observing neuronal outgrowth from the neuroprobe into a cultured hippocampal slice has been delayed by technical difficulties associated with staining the probe neurons. We have made great progress in overcoming these problems, as described below, and expect to begin the characterization of probe neuron integration into cultured slices soon.

We have been using the lipophilic fluorescent dye, DiI, which stains living (or fixed) neurons brightly when it is incorporated into the cell membrane. Reports in the literature show that neurons remain stained and healthy for up to several weeks when labeled with DiI (Paramore, Turner et al., 1992). Our probes and neurochips must be coated with polylysine and laminin to ensure cell adhesion to the wells and proper outgrowth. As mentioned in the previous report, staining the neurons with a DiI solution after they have been placed in the wells and begun to grow results in an unacceptable level of background staining of substrate. This background is transferred to neurons in the slice when the probe is placed in contact with the slice, making observation of the labeled probe neurons difficult or impossible. For this reason we have focused our efforts on developing a procedure to stain dissociated hippocampal neurons in suspension, before they are placed into the probe wells.

A major breakthrough was inspired by the voltage-sensitive dye literature. Voltage-sensitive dyes, like DiI, stain neuronal membranes. Because membrane dyes are lipophilic, they are difficult to dissolve in an aqueous solution that is not harmful to the cells being stained. For instance, DiI (dissolved in dimethylformamide to 40 mg/ml) tends to precipitate in cell culture media at concentrations often used to stain cells in suspension (40 μg/ml). The precipitated crystals cause cell aggregation and immediate lysis. Staining with voltage-sensitive dyes has been facilitated by including the macromolecular surfactant, Pluronic F127 (BASF Corp.), in the dye solutions (Davila, Salzberg et al., 1973). Because it is macromolecular, the surfactant itself does not become incorporated into the cell membrane, but merely serves to keep the dye

soluble, and 'catalyze' its transfer to the cell membrane (Lojewska and Loew, 1986; Lojewska and Loew, 1987). Thus, with 0.0025% F127, DiI is easily dissolved at concentrations greater than 40 μg/ml, as indicated by the fact that such solutions pass easily through a 0.2 μm filter, which would be clogged by a DiI solution lacking F127. We now routinely include this surfactant in our dye solutions, resulting in brighter staining and no cell loss due to aggregation.

DiI has an alkyl tail that anchors it in the cell membrane. The most commonly used form of DiI, and the one which we have used until recently, has a tail 18 carbon atoms long, "DiI (C18)". St. John reported that for spinal motorneurons from rat embryos, DiI with a C12 tail resulted in substantially better cell survival than DiI (C18) (St. John, 1991). We stained dissociated hippocampal cells from E17 rat embryos with either DiI (C18) or DiI (C12), and plated them onto coverslips coated with polylysine and laminin. As shown in the chart below, in contrast to the findings with the spinal motorneurons, we observed poorer cell viability in cells stained with DiI (C12) than with DiI (C18). The discrepancy could have resulted from differences in our staining techniques; St. John labeled the motorneurons in vivo. We were encouraged, however, by the fact that the cells stained with the short-tailed dye were much brighter, with less dye confined to intracellular organelles than were the cells stained with the C18 dye. Because the C12 dye remains in the plasma membrane longer than the C18 dye, fine processes are more clearly visible.

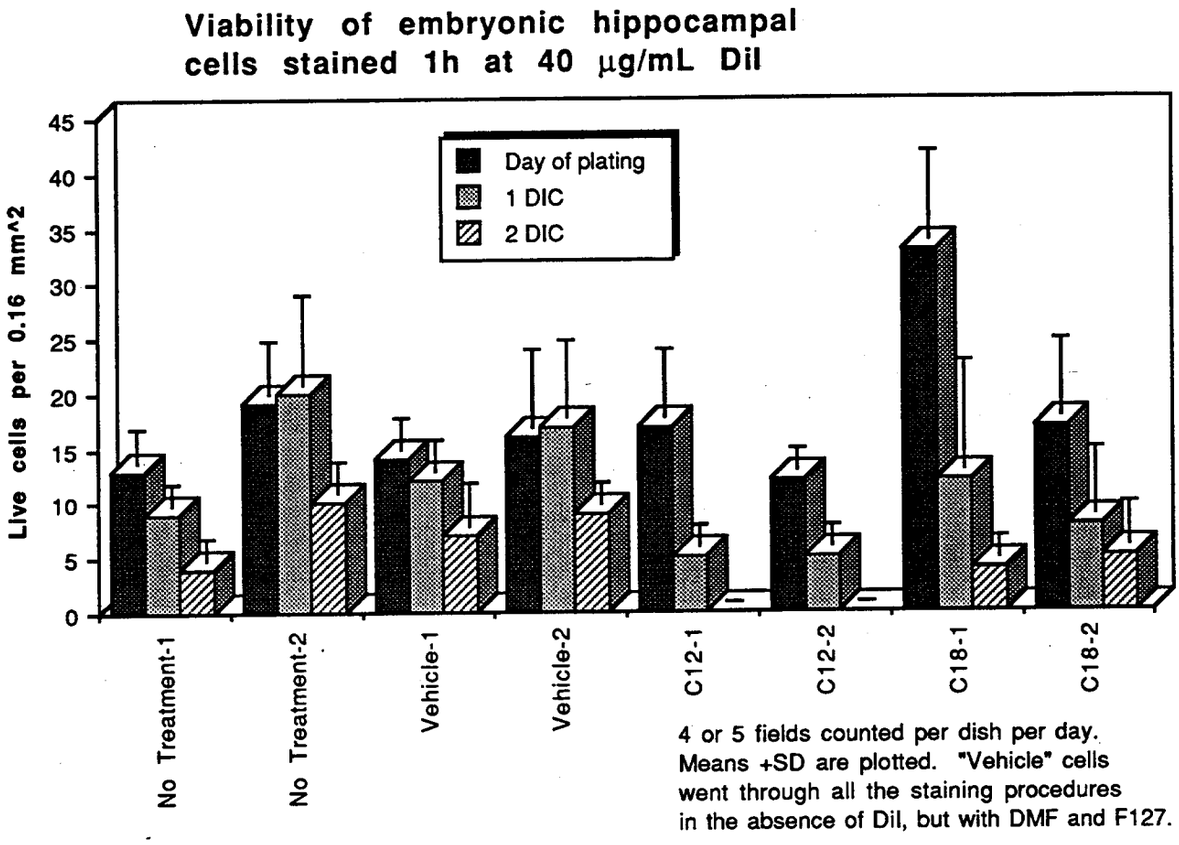

The lethality and brightness of the staining (for both types of dye) is roughly proportional to the time of staining and the dye concentration, so we are forced to accept a compromise in brightness that allows the cells to survive for enough time to observe outgrowth from the probe. A 15-min stain at 40 µg/ml DiI (C12) appears to produce good staining and little impairment of viability, compared to unstained control cells.

If dissolved DiI or stained debris are transferred to the probe along with the stained cells that are placed into the probe wells, then unwanted background staining of the slice will result. In order to reduce the amount of stained debris present, we now routinely filter cell suspensions through a 70 µm nylon mesh, which removes clumps of cells and other large debris. Then the suspension is centrifuged at 150 x g for 2 min, which pellets most of the cells, but leaves most of the small debris behind in the supernatant.

After staining, the cells must be separated from the dye solution by centrifugation and washing with fresh medium. Unfortunately, this process is fairly traumatic to the cells and can result in poor recoveries (<10%) of live, stained cells. To study this issue, we investigated the effect of centrifugation time on cell recovery, having observed that cells spun for longer times are much harder to re-dissociate. As shown in the graph below, at 150g, a spin time of 6 min provides the best recovery of cells from the pellet. We now use two rinses in 1-2 mL of medium, followed by 6 min spins at 150g.

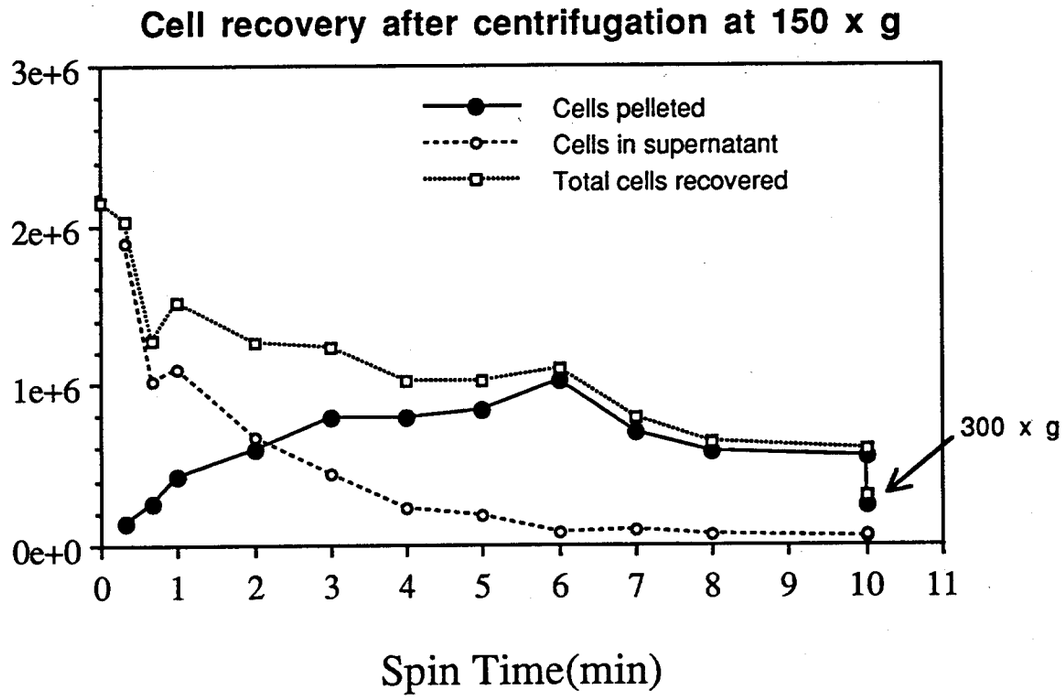

Another innovation in our rinsing protocol was the inclusion of a layer (~200 µL) of a sterile 5% solution of bovine serum albumin (BSA, in isoosmotic saline) underneath the dyed cell suspension while spinning. The cells easily sink to the bottom of the tube, but the dye solution is excluded, due to its lower density. Thus, after spinning, the dye solution can be almost completely removed without disturbing the pelleted cells. The BSA also seems to discourage clumping of the pelleted cells, making redissociation easier and less injurious. We routinely get cell recoveries of >75% using these enhancements.

Sucking and placing neurons

The traditional way to place cells into wells in our lab has been to add a few drips of a suspension of cells to a dish containing a probe (or neurochip) submerged in medium, and nudge the cells into the wells as they fall or soon after they land on the substrate. Because the above procedures for removing stained debris and dissolved dye are still not 100% effective, we have developed an alternative procedure that results in essentially no background staining of the probe with debris or dissolved dye.

We have prepared probe dishes by cutting a 12 mm hole in the center of a 35 mm plastic petri dish, and cementing a glass coverslip onto the underside of the dish, resulting in a central well 1-2 mm deep. The probe is attached to the coverslip with a tiny dab of silicone rubber cement, with its shank resting on a piece of silicon wafer that is also glued to the dish. This central area of the dish, including the probe, is then coated with polylysine and laminin, while the surrounding plastic substrate is not. The dishes are rinsed and the central well is filled with medium, covering the probe. Then, to fill the wells with stained cells, a drop of a suspension of cells is placed not in the pool of medium, but on the dry, uncapped plastic next to the pool.

The cells are then individually sucked up with a micropipet attached to a micromanipulator, and transferred to the probe wells. With a large-mouthed micropipet (100 μm opening), one has sufficient control of sucking and expelling to place the neuron gently over the center of a well, and it usually falls into the well within a minute. The lack of a coating on the plastic where the cell suspension was placed makes the cells easier to suck up if they have already touched down. This sucking and placing process does not appear to be harmful to the cells at all, and results in an undetectable level of background staining. The photos below are phase contrast and fluorescence micrographs of a stained neuron placed onto a numbered grid dish by this technique on the previous day.

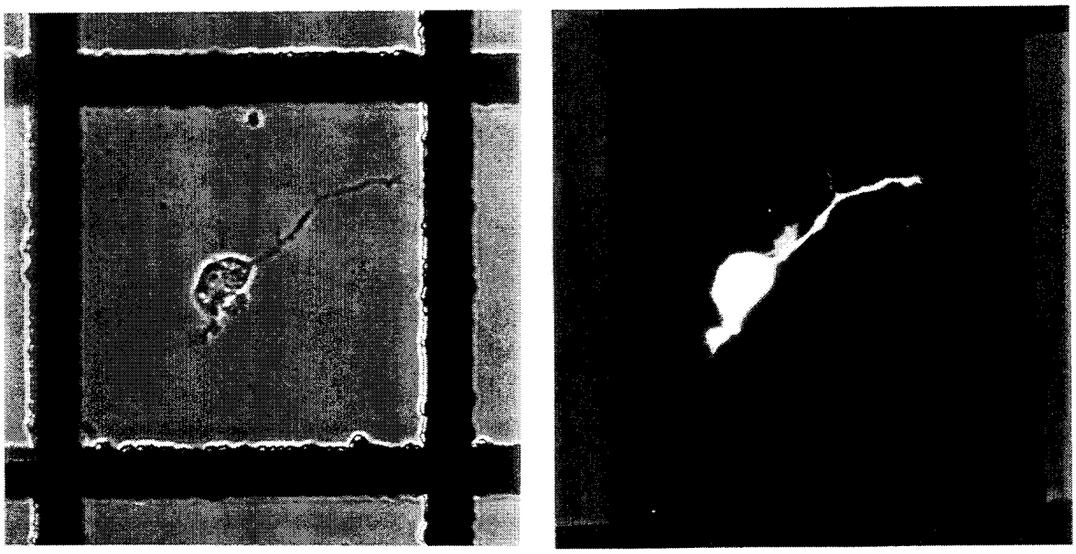

Summary

We have improved the brightness of staining through the use of the macromolecular surfactant, Pluronic F127, which also reduces cell aggregation and death during staining by preventing dye precipitation. We have enhanced the visibility of fine processes over time by switching to a dye with a shorter alkyl tail, DiI (C12). We have reduced contamination from stained debris by centrifugation and filtering of cell suspensions. We have improved the removal of the dye solution with the use of a layer of 5% BSA during centrifugation. And finally, we have eliminated the effects of any remaining background stain by transferring stained cells individually from one drop to another with a micropipet.

High-speed videography

We have completed construction of the 2nd generation high-speed CCD camera that will be used to image the electrical activity in neurons on the neurochips and in organotypic hippocampal slices, using voltage-sensitive fluorescent dyes. This improved design will allow the selection of arbitrary groups of pixels to be digitized by the computer. By discarding pixels over uninteresting regions of the image, we will be able to attain frame rates of at

least 1000 frames per second. The LabView programming to control the pixel selection, integration time, and other programmable parameters, has been completed and we are now busy testing the electronics of the camera.

References:

Davila, H. V., B. M. Salzberg, et al. (1973). "A large change in axon fluorescence that provides a promising method for measuring membrane potential." Nature **241**: 159-160.

Lojewska, A. and L. M. Loew (1986). "Pluronic F127: An effective and benign vehicle for the insertion of hydrophobic molecules into membranes." Biophysical Journal **49**: 521a.

Lojewska, Z. and L. M. Loew (1987). "Insertion of amphiphillic molecules into membranes is catalyzed by a high molecular weight non-ionic surfactant." Biochimica et Biophysica Acta **899**: 104-112.

Paramore, C. G., D. A. Turner, et al. (1992). "Fluorescent labeling of dissociated fetal cells for tissue culture." Journal of Neuroscience Methods **44**: 7-17.

St. John, P. A. (1991). "Toxicity of "DiI" for embryonic rat motoneurons and sensory neurons in vitro." Life Sciences **49**: 2013-2021.

Fabrication

In the past two quarters, multiple fabrication runs have been completed. With each completed wafer we have improved and modified the fabrication process to the point where the yield and quality of the chips produced are more than satisfactory. Several minor problems have been identified and corrected. A number of fabrication options have been created which allows the material used to create the grillwork to be either the original B-doped silicon or LPCVD nitride, LTO, thermal oxide, or PECVD nitride. The impetus behind providing these options is that for die recording it was considered preferable to have transparent grillwork to limit the amount of light lost in the system and thus improve signal to noise ratio. Also shown during this time period is the natural ability of the process to permit the fabrication of arbitrarily shaped probes and probe arrays. The work that is perhaps most significant and which is expected to greatly improve the amount of neuronal outgrowth from the wells is that which led to the conclusion that the amount of overhang present around the perimeter of the neural wells can be large enough to impede the outgrowth of processes and perhaps even prevent it completely. Once this problem was identified and proven to be a major reason that the *in vitro* results have been less successful than expected, a new fabrication process was developed and dummy chips produced with a new grillwork process.

Since the last report, several more metallized flat-bottom neurochip runs have been completed. The results of the last run show that the fabrication process has matured to the point where the quality (with one exception to be explained later) and yield of chips is now within an acceptable range. The grillwork of the resulting dies were more substantial than normally produced prior. This is due to better photoresist exposure at the bottom of the main cavity and improved RIE etching. Front-to-back alignment is almost perfect on these chips. The electrodes are centered in the grillwork pattern as desired and any misalignment is imperceptible. This success occurred with several wafers so we are confident that we have a repeatable results. The one disappointing point about these chips is that neuronal outgrowth was minimal and the reason why was not evident.

During this time, it was proposed that a transparent grillwork material was desirable in order to faciliatate voltage-sensistive dye recording of neuron activity. The reasoning for this is that, if we assume that the grillwork covers about 50% of a neural well, then by using an opaque material, 75% of the possible fluorescent dye-recording light is lost. First, 50% of the excitation light is blocked from entering the well and striking a stained neuron. Then, 50% of the fluorescing light produced by the dye is trapped within the well. By creating transparent grillwork, a factor of 4 increase in light can be achieved, greatly improving signal to noise ratio. Then, more reliable recordings can be had, or the staining level of the cells can be reduced to improve culture survivability.

As a proof of concept, a run of dummy chips with transparent grillwork was produced. One set was created with LPCVD nitride as the grillwork material and the other used wet thermal oxide. After fabrication, neurons were implanted and grown in an attempt to investigate the improved SNR of the transparent material. However, another much more important piece of information was discovered. The success rate for neuronal outgrowth from the two types of chips was markedly different: neurons were much more successful in the oxide chips than in the nitride. Since previous work has shown that neurons grow equally well on nitride and oxide surfaces, the difference was not believed to be caused by incompatibility between the neurons and the grillwork material. Thus, an alternative explanation was sought.

It turned out that the geometries of the two types of wells created in this run were slightly different. For the nitride chips, overhang around the perimeter of the chip was constant at about 1μm. The amount was slightly greater at the corners due to rounding of the features in the exposure step. Because the grillwork was created with a plasma etch, the features were well defined and constant from well to well and from die to die. This was not the case with the thermal oxide chips. The grillwork on these dies were created by a wet etch process which etched the oxide isotropically. As a result, instead of sharp straight lines and minimal photoresist undercut, the features became large, rounded structures. Another feature, found in SEM pictures taken later, was the presence of a very thin, optically invisible layer of oxide (< 200Å) extending from the sides of the features out several microns towards their centers. This feature can be seen in the image below"

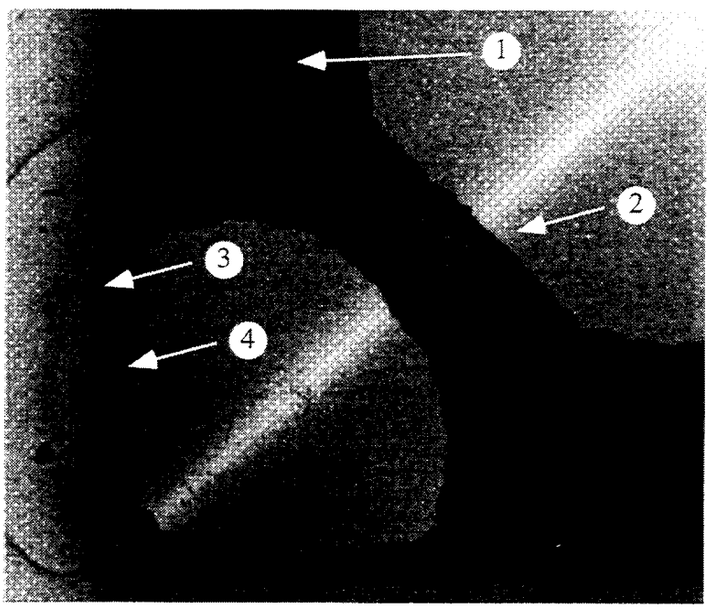

1) Thick oxide from which grillwork was fabricated.
2) Ultra-thin oxide forming a grillwork bar.
3) The transistion from dark to light indicates the edge of the well.
4) Ultra-thin oxide forming the overhang around the perimeter.

The undercut resulting from EDP etching extended underneath this thin oxide but in many wells did not reach the thicker oxide surrounding it. After the EDP etching step, patches of the thin oxide on many of the wells were broken due to normal handling and cleaning of the dies. The overall result was the production of wells whose perimeter had areas where there was zero overhang of the grillwork material. It was then proposed, and has since been proven, that the amount of overhang produced by the original fabrication process is too great to permit adequate neuronal outgrowth for *in vitro* studies.

To confirm that the amount of overhang present around the wells of the completed, metallized chips and probes was indeed large enough to impede neuronal outgrowth, a series of SEM samples were created revealing the wells in cross section. SEMs of the well's cross section have been desired since they were first created but all previous attempt to create the necessary samples have been unsuccessful. In this study we successfully cross sectioned wells from flat

bottomed neurochips and from completed neuroprobes. What we found was both gratifying and disheartening. In both cases, the information gleaned was very enlightening.

In the case of the neuroprobe wells, all of the expected features were present proving that, overall, the fabrication process is a success. For the first time, SEMs of the dimple at the bottom of the well have been taken. As desired, the intricate and demanding initial processing steps have created an ≈ 0.8μm deep depression at the bottom of the neuron wells with a gold electrode at its center. The bottom of the well is ≈ 6μm square and the silicon beneath the grillwork is completely removed. The amount of overhang around the well's perimeter is ≈ 0.5μm. One view is shown below:

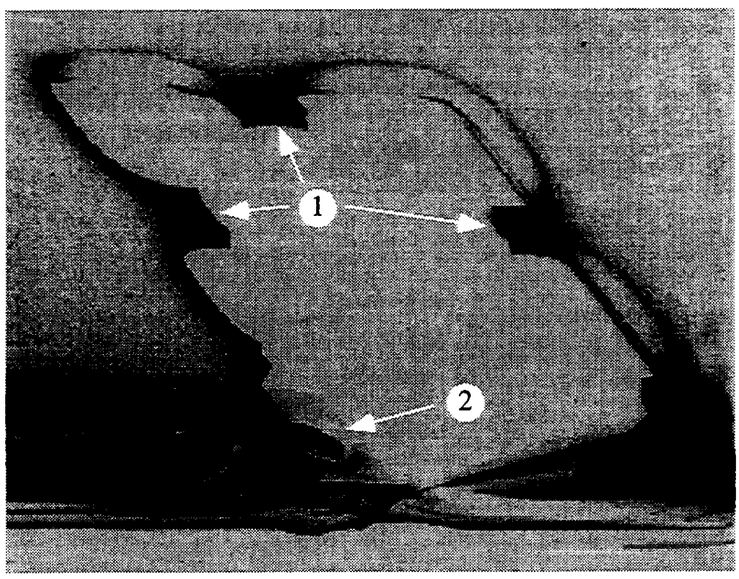

1) Broken B-doped grillwork.
2) 0.8μm deep dimple at bottom of neuron well.

The SEMs of the flat-bottomed chips are quite different. As desired, the bottom profile of these neuron wells are perfectly flat with a gold electrode at the center. The grillwork on these chips is very well defined and quite thick at ≈ 3μm. Unfortunately, the most notable feature of these wells' cross sections is also the most distressing. Instead of having sidewalls which slope down from the grillwork to the well's floor at a 54° angle, these wells have a "hexagonal" shape. The amount of "hexagonal" distortion varies from well to well. Some

show no such distortion. Most show at least some. The SEM below shows one of the more extreme cases. It should be noted that such symmetry is rare. Most of the distorted wells showed little distortion on one side and gross distortion on the other. This is evidence that the RIE does not etch the grillwork uniformly, even on a per well basis.

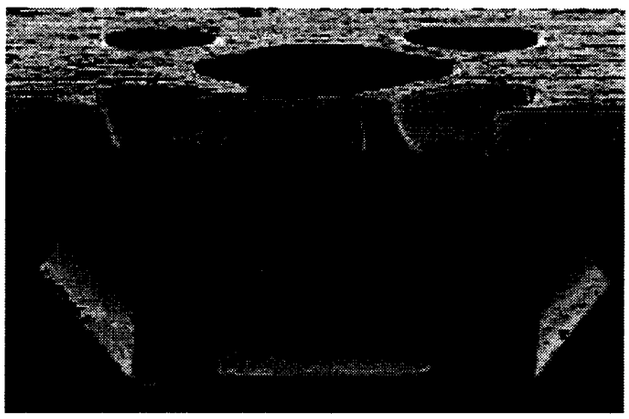

The cause of this unique and unexpected shape can be traced back to the step in which the RIE is used to etch the B-doped silicon to define the grillwork. This step has historically been one of the more demanding steps in the process. To be successful, first the grillwork must be patterned using photoresist and the stepper. For sharp features, it is desirable to use as thin a photoresist as possible. The thickness sought is determined by how thick the resist must be to withstand the RIE etch which defines the grillwork. The actual thickness used is determined by how uniform the resist can be spun at the bottom of a 3mm x 9mm x 500μm deep cavity. Through experience, we have been able to expose and develop the resist such that the resulting features, while not perfect, are still very good. The results from the RIE are a little less predictable.

After the resist is patterned, approximately 3μm of the exposed B-doped silicon must be etched using the RIE. The desire is to etch only the B-doped silicon, stopping at the doped-undoped silicon interface. After an EDP etch, the resulting well is as desired and has minimal overhang around its perimeter. In practice, stopping the RIE etch at the doped-undoped interface can never be achieved and a small amount of overetching must occur if the corners of the features are to be successfully defined as shown in the figure at left below. This

increases the amount of overhang produced after by the EDP etch slightly to an amount that should still allow neuronal outgrowth but which is nearing the tolerable limits. The figure at right below shows the expected geometry:

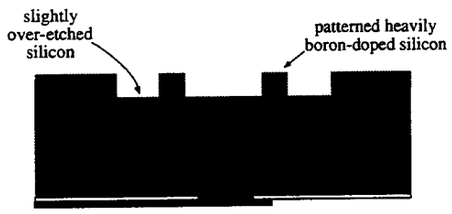

RIE overetch into undoped silicon

Resulting geometry after EDP etch

In recent runs, however, the etching at the center of the features has been significantly greater than at the corners. The result is that the etch at the center has extended a significant distance down into the undoped silicon as shown in the figure at left below. EDP etching of such a structure results in the hexagonal shaped wells shown in the figure at right, which our SEM studies have shown to be the true geometry of many of the fabricated wells.

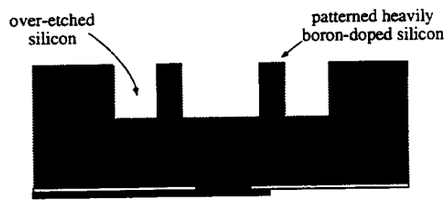

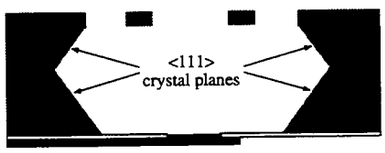

RIE overetch into undoped silicon

Resulting geometry after EDP etch

A new process for the creation of the grillwork was devised, which guarantees that there will be no overhang of the grillwork material around the perimeter of the well. The process no longer uses the B-doped silicon as anything more than an anisotropic etch stop. Once the main cavity is created, the B-doped silicon is selectively etched from the basin and a layer of LPCVD nitride deposited. This nitride is then patterned using a plasma etch so that only the shape of the grillwork for the neuron wells is left. A secondary benefit of removing almost all of the nitride from the bottom of the cavity is that the effects of its stress on the thin membrane are removed. The next step is the growth of a thin layer of thermal oxide followed by its patterning. The mask used consists simply of an array of squares which define the size of the tops of the neuron

wells. The exposed oxide is stripped with buffered HF and the wells formed using EDP. The result are wells with oxide overhanging their perimeters. This overhang is then easily removed using a second buffered HF etch which removes the oxide. The final geometry has nitride grillwork covering a trapezoidal shaped well that is guaranteed to have no overhang around its perimeter. The three figures below diagram this process:

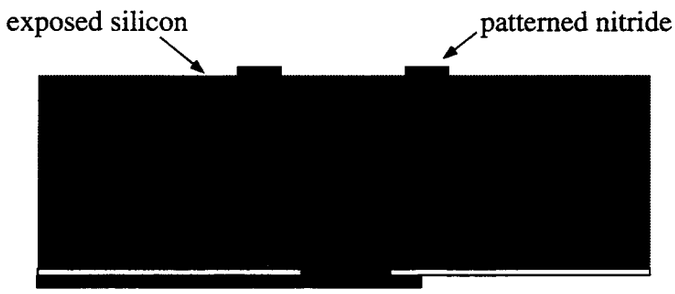

Pattern nitride leaving only the grillwork bars

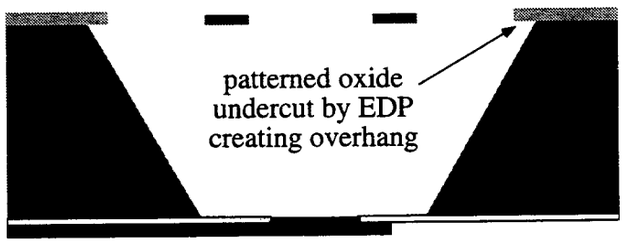

Grow oxide, pattern well opening and EDP to create well

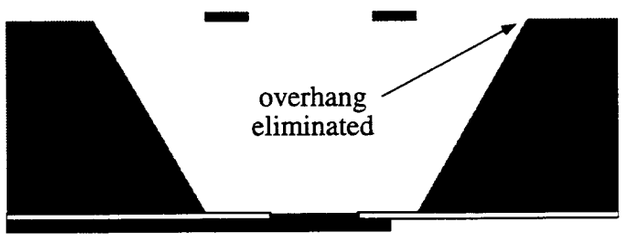

Strip oxide removing any possibility of overhang

At present, only dummy chips using this new process have been created. A run of dummy neuron probes is presently being fabricated. The grillwork design has been modified to leave smaller corner openings, since neurons have been seen to escape from wells through the corners. One of the drawbacks of this process is that it requires that the metallization of the dies be

done after the main cavity has been formed. This means multiple processing steps must be conducted on the thin, fragile membrane. Past experience has proven that this can be done successfully but, as can be imagined, much greater care must be exercised to ensure that the wafer is not broken. A beneficial point to metallizing the wafer after the wells have been created is that the wells themselves can be used as the front-to-back alignment marks ensuring perfect alignment. The SEM below shows the new neuron wells with zero overhang.

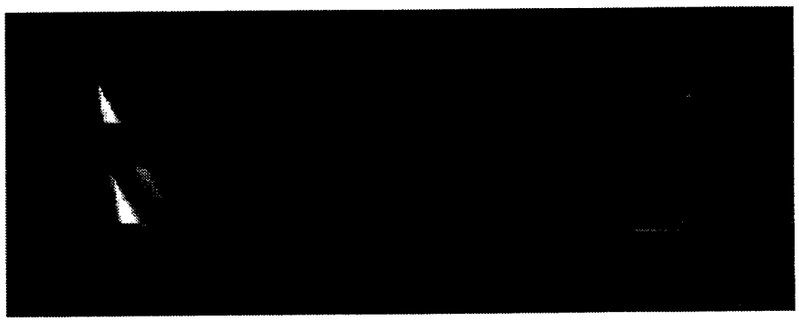

While waiting for the present dummy neuroprobes to be produced, we felt it necessary to remove the overhang from some of the previously fabricated probes so that work at Rutgers could continue. Two techniques were employed, to varying degrees of success, to accomplish this. The first involved placing glass micro-beads over the wells and etching the probes in the RIE. The beads were selected such that there size was large enough to cover the grillwork over the center of the wells yet small enough to leave the corners unprotected. The RIE etch then removed all of the grillwork material from the probes except for the grillwork itself eliminating the overhang around the perimeter. This method was abandoned due to the difficulty in selecting the properly sized beads and placing them over the wells an effort made more difficult by the fact that they hold a charge and tend to be repelled from surfaces. The second method involves coating the probes with photoresist and then scratching that resist away so as to reveal the corners of the wells. The exposed nitride is then removed in the RIE. As with the bead method, this involves very fine work and is quite time consuming. Due to the dimensions involved and the tools used, typically a maximum of two corners per well can be exposed. Still, the process worked and several probes were prepared using this technique.

The final bit of work completed since the writing of the last report was the fabrication of arbitrarily shaped probes, and demonstration of how such probes can be stacked to create a three dimensional neuroprobe array. Because we use an RIE vertical etch to define the shape of our probes, they can be fabricated into any continuous shape. Other techniques, such as anisotropic etching, that could be used to define the probe would limit the realizable shapes. To show how extreme the shapes can be, we created 1 x 3 arrays of serpentine probes. By designing these probe sets with different sized bases, they can be stacked to create the three dimension neuron probe arrays shown below.

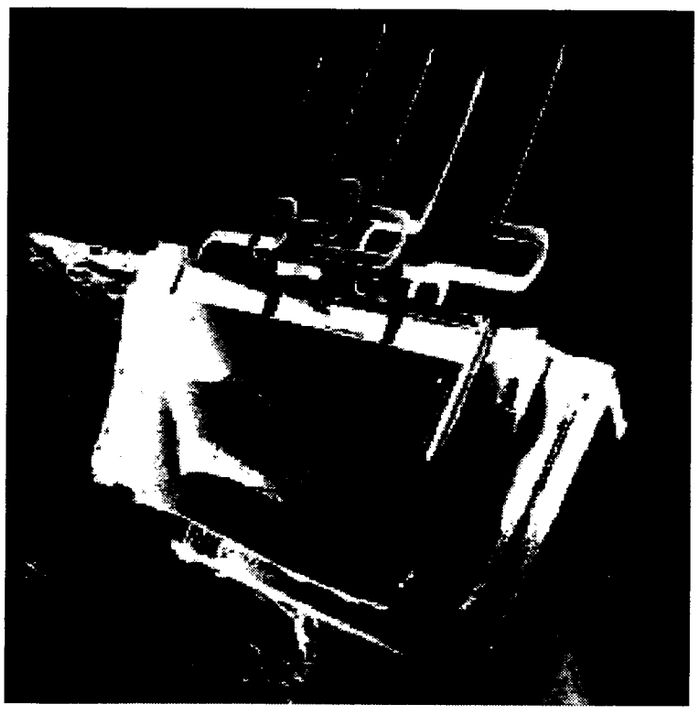

In Vivo Studies

Summary

1. During this period we continued to analyze the data from silicon probes containing cultured septal neurons transplanted into hippocampus of adult rats with fimbria fornix lesions. In addition to six rats which were analyzed during the previous period (1-2 months after transplantation of silicon probes) we have performed the AChE reaction on another five rats 4-6 months after transplantation. In two of the five rats cholinesterase-positive fibers were revealed in the vicinity of the silicon probes.

2. Transplantation of DiI-stained hippocampal neurons was done on four rats. The analysis revealed that stained cells could be detected one month after transplantation. However, particles of DiI were also observed in and around the graft, making the interpretation difficult. Although we followed a protocol which proved efficient for labeling neurons *in vitro*, it appears that more extensive washing is necessary for *in vivo* grafting.

Results

About 400 neurons were moved into wells of 34 probes. As in previous experiments we reused at least half of the probes using the protocol developed recently in Pine's Lab. We have chosen 0.1% and 1.0% of poly-L-lysine for covering surface of the probes. NBM/B27 Medium was used for culturing. After placing neurons into wells, we waited at lest 60 minutes to allow them to attach. The pH was kept constant by flowing 10% carbon dioxide over the mdeium. Next, the probes were transferred into an incubator. We did not observe outgrowth of processes after 24 hours, but could detect neurons within the wells.

Twenty-two probes were transplanted into hippocampi of five rats with preliminary fibria-fornix lesion. Four to six months after transplantation the brains were cut and sections were stained to reveal AChE fibers using a modified Karnovsky-Roots staining.

One rat was rejected from analysis because of incomplete fimbria-fornix lesions. In two animals no AChE positive axons were found. In the two remaining rats axon collaterals were clearly identified in hippocampi where probes were implanted. In one rat, the density of AChE fibers was fairly high. Examples of AChE fibers together with a silicon probe are shown in the figures on the following page. Pictures B and C are of the upper and lower parts of the probe shown in A.

Transplantation of an embrionic hippocampal cell suspension stained with DiI into hippocampus of adult rats

To examine whether cells stained with DiI are able to survive within the host brain, we carried out experiments with low density cell grafts but without silicone probes.

Staining procedure.

1. DiI stock solution (40 mg/ml DiI/DMF + 2.5% pluronic F127) and 2 ml serum free Neurobasal/B27 were warmed in 37°C water bath.
2. 1 µl warmed DiI stock solution was pipetted into 2 ml warmed media.
3. Suspension from six-eight hippocampi of 17 day rat embryos was pipetted into stain media.
4. The tube with suspension was placed into incubator for 60 min, and swirled every 5-10 min.
5. The tube with suspension was centrifuged at 200 g for 3 min.
6. Supernatant was pipetted off, 1 ml Neurobasal/B27 medium was added a cell pellet was resuspended.
7. Steps 5 and 6 were repeated and cells were left at room temperature after additional centrifugation till transplantation.

Transplantation procedure.

Sprague-Dawley rats were anesthetized with mixture 4 mg/kg of ketamine (25 mg/kg), xylazine (1.3 mg/kg) and acetopromazine (0.25 mg/kg)


B


C


A

and held in a stereotaxic frame. 0.3-0.5 mm^3 of suspension taken from a neuron pellet were transplanted in the left and right hippocampi by a microsyringe after opening the skull.

For observation of the transplants the rats were deeply anesthetized and perfused with 200 ml of saline followed by 10% of buffered formaline 4 to 6 weeks after transplantation. Then brains were cut on a vibratome in 60 μm sections and examined with a fluorescent microscope.

Results

Two rats with four grafts were observed 4-6 weeks after transplantation. The transplants were observed in all cases. All of them had a volume of 0.5 mm or less and contained stained neurons. The outgrowth of short processes into the host brain was observed. However, small (about 20-30 μm) crystals of DiI were observed also, within transplants and on the border with the host brain. Retrograde staining of host neurons was also observed. Such contamination made detailed interpretation of the data impossible.

We believe that crystals within the grafts are a result of a high density of suspension. In future experiments, more careful washing of suspension after staining is required to deplete all crystals.

Appendix: PID Temperature Controller

Several methods are available for controlling temperature. Three elements are always required: a method of transducing sample temperature, a means of supplying heating or cooling power to the sample, and a feedback mechanism. The most elegant and robust class of feedback mechanisms is the Proportional-Integral-Differential (PID) method. The sample temperature is transduced to a voltage signal $V(T)$, which is then compared to an adjustable set voltage V_{set}, generating the signal $\Delta V = V_{set} - V(T)$. The set voltage normally corresponds to the transduced voltage at the desired temperature T_{set}. An output voltage V_{out} is supplied to a heater resistor thermally connected to the sample. After suitable and tunable gains, V_{out} contains terms Proportional to ΔV, to the time Integral of ΔV, and to the time Derivative of ΔV. The PID is essentially a general class of devices, containing the simple proportional temperature controller and the simple on-off type of controller. Controllers with all three PID terms, once properly tuned, have the following advantages.

(1) Vanishingly small offset error at equilibrium, set mainly by the leakage time constant of the integrator capacitor, which can be hundreds of hours.

(2) Very robust and predictable response, even with order-of-magnitude changes in heat load and desired temperature. This also implies that the tuning requirements are very flexible and forgiving, and that the same controller can be used with minor adjustments for a wide variety of systems.

(3) Completely independent operation, no operator input is required.

(4) Relatively fast response time, dependent upon the inherent time constant of the system.

Basic Theory of Temperature Control

All temperature control systems must account for the inevitable non-idealities of heaters. These include time lag between heat input and diffusion to the temperature controller, differences in static and dynamic temperature between sample and sensor, variable heat leak to the environment, heat capacities of the components, and the temperature dependence of the heating element.

Table A.1. A list of variables used in the analysis.

$\dot{H}$	heat supplied by the resistor
$\dot{h}_1$	heat lost by the resistor directly to the environment
$\dot{h}_2$	heat passing into the sample
$\dot{h}_3$	heat load
T	sensor temperature
T_R	temperature of heater resistor
T_0	temperature of the environment
σ_1	heat conductance from resistor to environment
σ_2	(low) heat conductance between resistor and block
σ_3	conductance of heat load
V_R	output voltage of controller placed across heater resistor
R	heater resistance
C	heat capacity of block

A resistor supplies heat at the rate

$$\dot{H} = \frac{V_R^2}{R} = \dot{h}_1 + \dot{h}_2, \tag{1}$$

The heat has been broken into two terms: heat lost immediately to the environment, and heat passing through the low-conductivity path to the heater block. The heat flow from the heater to the environment and to the heater block are:

$$\dot{h}_1 = \sigma_1(T_R - T_0) \approx A\dot{H} \tag{2}$$
$$\dot{h}_2 = \sigma_2(T_R - T) = C\dot{T} + \dot{h}_3.$$

To first order, the radiative heat lost to the environment from the resistor is simply proportional to the total heat supply, and A is a constant. Heat going into the heater block has two paths: warming the whole thing up through its' heat capacity, and radiative heat loss to the environment.

It is now necessary to make a weakly justified assumption in order to simplify the math. In equation (1), the heat supply varies as the square of the applied voltage. However, we are going to be writing differential equations involving the applied voltage. Squaring the applied voltage will introduce non-linear terms, which greatly complicates the solutions and obscures the dependencies. Generally, non-

linear differential equations must be solved numerically, which means that an analytical solution (that is, a simple equation describing the behavior) does not exist. Since we will be dealing with relatively small changes (i.e. less than an order of magnitude) in applied voltage, and we are not interested in exact solutions, it is reasonable to express the heat supply as a linear function of the applied voltage:

$$(1-A)\dot{H} = BV_R, \tag{3}$$

where B is taken to be a constant (but is, in a strict sense, linearly dependent upon V_R). This approximation will be sufficient for our purposes, since shifting from a quadratic to a linear dependence preserves the main features of the function in the region of interest. This approximation would not be valid if we were interested in both positive and negative V_R, since heat is supplied to the resistor in both polarities, while the linear dependence in Equation (3) suggests that the resistor would be cooled if the voltage were negative. The approximation also would be invalid if Equation (1) were pathological (meaning that divergences exist in the region of interest). Inserting Equations (2) and (3) into Equation (1) yields:

$$BV_R = C\dot{T} + \sigma_3(T - T_0). \tag{4}$$

Now we will assume a temperature controller with differential, integral and proportional terms. We have:

$$V_R = r\Delta T + s\int \Delta T dt + w\Delta\dot{T}, \tag{5}$$

where r and s represent the adjustable but constant transduction and gain of the difference and integral terms, and $\Delta T = T_{set} - T$. Inserting into Equation (4):

$$Bw\Delta\dot{T} + Br\Delta T + Bs\int \Delta T dt = C\dot{T} + \sigma_3(T - T_0). \tag{6}$$

Differentiating to eliminate the integral yields:

$$Bw\Delta\ddot{T} + Br\Delta\dot{T} + Bs\Delta T = C\ddot{T} + \sigma_3\dot{T}. \tag{7}$$

Now, since $\Delta T = T_{set} - T$, differentiating gives $\Delta\dot{T} = -\dot{T}$. That is, increases in the temperature cause ΔT to become smaller. If the temperature is below the set point, and the temperature rises, then the error temperature ΔT gets smaller (closer to zero). Expressing Equation (7) in terms of ΔT gives:

$$\begin{aligned} &Bw\Delta\ddot{T} + Br\Delta\dot{T} + Bs\Delta T = -C\Delta\ddot{T} - \sigma_3\Delta\dot{T}, \\ &(Bw + C)\Delta\ddot{T} = -Bs\Delta T - \Delta\dot{T}(\sigma_3 + Br). \end{aligned} \tag{8}$$

Damped Harmonic Oscillator

Equation (8), by design, looks exactly like the differential equation for a damped harmonic oscillator, that is, a mass on a spring in molasses (or a shock absorber). If you are not particularly interested in the gory mathematical details, you can skip down to the section below marked by stars to read about the solution and what it means. Such a system has the following differential equation to describe the motion:

$$m\ddot{x} = -kx - \gamma\dot{x}. \tag{9}$$

Here, m is the mass, x is the position of the mass, k is the spring constant, and γ is the damping term. The left-hand-side of this equation represents the acceleratioon of the mass due to the forces exerted on it, which are the two terms on the right-hand-side. Two forces are given. The first is the restoring force due to the spring, Hooke's Law. If the mass is pushed to positive x, this force acts to accelerate the mass back to x=0. If the sign on this term were positive, the mass would be stable at $x = 0$, but the smallest perturbation would cause the mass to go flying away, faster and faster the farther away it gets. The second is the viscous damping term. "Damping" is a very loosely defined concept, and it depends on many things, including the shape of the object, the speed, turbulence, the specific medium doing the damping, etc. For most materials at low speeds, the damping is linearly related to the relative speeds involved. The sign here is also negative, since any velocity $\dot{x}$ causes the mass to be decelerated.

This equation can be solved by assuming the solution $x = x_0 \exp(pt)$, where x_0 and p are (possibly imaginary) constants to be determined. Differentiating this solution with respect to time yields:

$$\begin{aligned} x &= x_0 \exp(pt) \\ \dot{x} &= x_0 p \exp(pt) = px \\ \ddot{x} &= x_0 p^2 \exp(pt) = p^2 x. \end{aligned} \tag{10}$$

The velocity and acceleration terms are just linearly related to the position, which is why this solution works! Substituting these expressions into Equation (9),

$$\begin{aligned} mp^2 x &= -kx - \gamma px \\ mp^2 &= -k - \gamma p. \end{aligned} \tag{11}$$

Notice that all references to the constant x_0 have dropped out of this equation. If necessary, x_0 can be determined using the initial conditions of the particular setup, and the constraint that x is necessarily a real quantity. Using the binomial expansion to solve this equation for the roots of p gives:

$$p = \frac{-\gamma \pm \sqrt{\gamma^2 - 4mk}}{2m} \qquad (12)$$
$$= \frac{-\gamma}{2m} \pm i\sqrt{\frac{k}{m} - \frac{\gamma^2}{4m^2}}.$$

☆ ☆ ☆ ☆

We can then write the general solution as:

$$x = x_0 \exp\left(-\frac{\gamma}{2m}t\right)\exp(\pm i\omega t), \qquad \omega = \sqrt{\frac{k}{m} - \frac{\gamma^2}{4m^2}} \qquad (13)$$

This nasty-looking expression is best understood by considering its individual components. The first exponential is always negative, indicating a decay with a time constant $2m/\gamma$. A heavy mass, or a low-viscosity fluid like air, leads to a large time constant, meaning that it takes a long time to settle down. A light mass or a high-viscosity fluid like molasses gives a short time constant, so that this exponential settles quickly.

The second exponetial contains the oscillatory component. Let's consider the situation where we pull our springed mass away from its equilibrium point and let it go. If ω is real, that is, if the system is underdamped and $\gamma^2 < 4mk$, then the system will overshoot the equlibrium point and oscillate about its equilibrium point before settling in, just like a pendulum. In considering the solutions to a differential equation, it is usually useful to consider the extreme cases. If there were no damping, and $\gamma = 0$, then the exponential has an infinite time constant: it never damps out, it would swing forever. We would also return to the classical harmonic oscillator solution, with the frequency $\omega = \sqrt{k/m}$.

Let's take that pendulum and dunk it in oil. If you were to set the pendulum swinging now, it would slowly ooze down to the bottom of its swing and stop. This is the case where the system is overdamped, and $\gamma^2 > 4mk$. Then, the frequency ω becomes imaginary, and there is no oscillation at all. The damping time constant becomes:

$$\tau_{\pm} = \frac{2m}{\gamma \pm \sqrt{\gamma^2 - 4mk}} \qquad (14)$$

There will be a sum of two exponential terms in the solution, with two different time constants. We can determine their relative sizes by assuming that we hold the mass still before letting go, and solving for zero velocity. We also need to know the initial starting position.

$$\dot{x}(t=0) = \frac{x_+}{\tau_+}\exp(-t/\tau_+) + \frac{x_-}{\tau_-}\exp(-t/\tau_-) = 0 \tag{15}$$
$$x(t=0) = x_+ \exp(-t/\tau_+) + x_- \exp(-t/\tau_-)$$

At t=0, this simplifies to:

$$\frac{x_+}{\tau_+} + \frac{x_-}{\tau_-} = 0 \tag{16}$$
$$x_+ + x_- = x(t=0).$$

If we consider the extreme, where $\gamma \to \infty$, then the two time constants are $\tau_- = m/\gamma \to 0$ and $\tau_+ = \gamma/k \to \infty$. The first expression in Equation (16) indicates that $x_- \to 0$ when $\tau_- \to 0$, so that the decay time constant is simply $\tau_+ = \gamma/k \to \infty$. What does this mean? Well, the mass takes forever to reach its equilibrium point. That's essentially what happens to glass when it sets. Glass is not crystalline, it's not solid. It's like really thick water. But the viscosity is so astronomically, immeasurably large that the glass never settles down to its equlibrium point, which would be a puddle on the ground.

We've considered the extreme cases, where the viscosity is very big and where it's very small. There is one more interesting case: critical damping. Look at Equation (13), describing the solution to the position of the oscillator. We know that the behavior is oscillatory at low damping (that is, ω is real), and that it decays exponentially at high damping (where ω is imaginary). What happens at the crossover point, where the frequency ω goes to zero? At this value of the damping, we have the fastest decay time constant with no oscillatory behavior. That means that the mass proceeds to its equilibrium point as quickly as possible, with no overshoot. We can solve for the damping constant necessary to give critical damping:

$$\omega = \sqrt{\frac{k}{m} - \frac{\gamma^2}{4m^2}} = 0, \tag{17}$$
$$\gamma = 2\sqrt{mk}$$

Thus, the time constant for the decay is simply $\tau = \sqrt{m/k}$, the same value for the period of the classical harmonic oscillator. This means that the mass proceeds rapidly to the equlibrium point and magically stops.

Analogy Between the PID Temperature Controller and the Harmonic Oscillator

Look at the differential equations for the temperature difference in the PID controller and the position of a harmonic oscillator (Equations (8) and (9)). There is an exact, one-to-one correspondence between the terms of these equations, summarized in the table below.

Harmonic Oscillator	PID Temperature Controller
Mass m	Heat Capacity and Derivative terms, $C + Bw$
Spring force kx	Integral term $Bs\int \Delta T\, dt$
Damping constant γ	Sum of heat leak and controller difference term, $(\sigma_3 + Br)$
position x	Difference between set and actual temperatures, $\Delta T = T_{\text{set}} - T$
Critical damping $\gamma = 2\sqrt{mk}$	Critical damping $Br = 2\sqrt{CBs}$
Critical damping time constant $\sqrt{k/m}$	Critical damping time constant $\sqrt{Bs/C}$

Differential terms are useful in systems where large, rapid temperature changes are required, so they have not been implemented in this system. Also, they tend to be rather small, so that a high gain is necessary, making it quite noisy. A further disadvantage is that the effect of a differential term is to increase the heat capacity, which is generally too large anyway. Alternatively, one could use a negative differential term, to reduce the effective heat capacity. This would tend to be a destabilizing effect, however.

Notice that the gain and transduction terms Bs and Br are present in the integral and difference. So, to tune these values, we need to know the parameters of the heater system. The way it's supposed to work is this: the difference term supplies heat until the system is near the desired temperature. Then the difference term is nearly zero, so the integral term takes over. If the system is exactly at the desired temperture, the difference term is zero, supplying no heat, and the integral term no longer changes (but is not zero!!). Just think of the spring analogy. At equlibrium, the mass isn't moving, so the damping force vanishes and the spring maintains a steady displacement to counteract gravity.

In the temperature controller, we want to maintain the cell culture at 37 °C. We'll always be warming up from room temperature, and we definitely don't want to overshoot 37 °C. So, we want the system to be critically damped, but we also want to err on the side of overdamping to avoid overshooting. Figure 1 on the following page illustrates the behavior of the temperature with varying amounts of damping. Too little damping, only by a factor of 4, causes severe oscillations in temperature, compared to critical damping. The temperature swings lose about half their amplitude in each cycle, and take a LONG time to

dampen away. On the other hand, overdamping merely causes the system to slowly ramp up to the proper temperature. Since we'll be trying to maintain a set temperature for many hours, that's not such a bad sacrifice. Obviously, we'd like to be as close as possible to critical damping, though.

The temperature transduction is performed by an AD590, a thermistor-based device which acts as a current source, putting out 1 μA/Kelvin. A resistor array converts this into a voltage signal giving 10 mV/°C. Typical small heaters in our lab have a 20 Ω resistance and require about 5 V to maintain 37 °C. The older style of heaters were glued together with silicone rubber, an excellent heat insulator, and caused a large time lag between the addition of heat and a temperature change in the block. These heaters took about 10 minutes to go from room temperature to 37 °C. Using nichrome wire epoxied in close, electrically isolated contact as a heating element, this time can be potentially reduce by a factor of 2-3. These numbers suggest that the integrator term should go from 0 to 5 V over 10 minutes, with an average signal size of $5\,°\mathrm{C}\cdot 10\ \mathrm{mV}/°\mathrm{C} = 50\,\mathrm{mV}$. Thus, we need an integrator with a time constant of:

$$\frac{5\ \mathrm{V}}{50\ \mathrm{mV}}\cdot \mathrm{gain}\cdot RC = 100\cdot \mathrm{gain}\cdot RC = 600\,\mathrm{sec}. \tag{18}$$

This is an awfully long time constant for a solid-state integrator, so we've minimized the gain as much as possible, to 0.5. This suggests a time constant of RC=12 seconds. With a large, 10 μF polyester film capacitor, this requires a resistor of about 1MΩ. Also. the integration term is:

$$s\int \Delta T dt \approx s\Delta\overline{T}\Delta t \approx 5\ \mathrm{V} \tag{19}$$

$$s \approx \frac{5\mathrm{V}}{5\mathrm{K}\cdot 600\,\mathrm{sec}}$$

Next, we can determine the proper damping gain for the proportional term, given by $Br = 2\sqrt{CBs}$. If the proper setting for R=20 Ω is $V_R \approx 5\mathrm{V}$, then $B \approx V_R/R \approx .25\ \mathrm{V}/\Omega$. Then we need a net gain for the proportional term of:

$$Br = 2\sqrt{CBs} \tag{20}$$

$$r = 8\frac{\Omega}{\mathrm{V}}\sqrt{100\frac{\mathrm{J}}{\mathrm{K}}\cdot\frac{1}{4}\frac{\mathrm{V}}{\Omega}\cdot\frac{1}{600}\frac{\mathrm{V}}{\mathrm{K}\cdot\mathrm{s}}}$$

$$= 1.6\frac{\mathrm{V}}{\mathrm{K}}.$$

Since the transduction gain is 10 mV/K, we need a net gain of around 160 to have the system critically- or over-damped.

Block Diagram of the Circuit

Below is a block digram of the PID controller circuit.

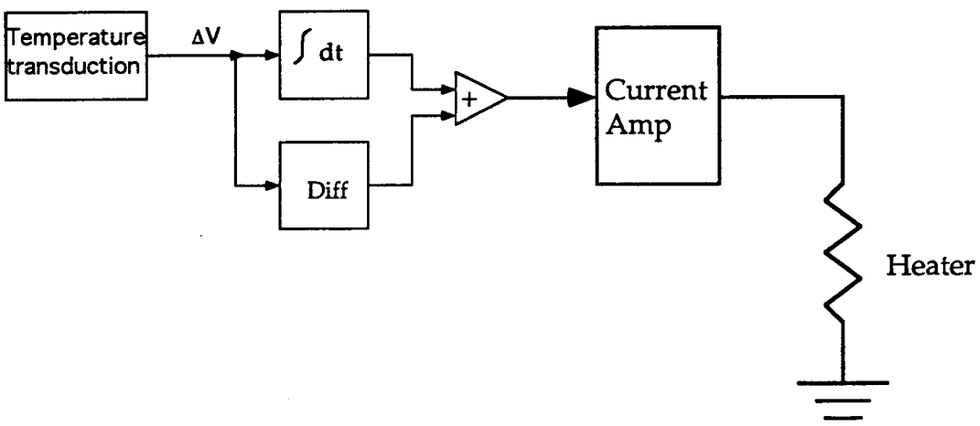

Time course of temperature with ideal PID controller at various settings of the damping constants.